Politecnico di Torino

Masters Degree in

Environmental and Land Engineering (Climate Change)

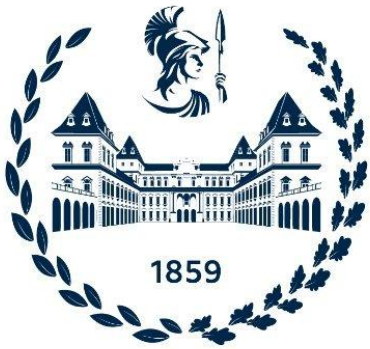

Master's degree Thesis

Impact of climate change on groundwater levels in the Iberian Peninsula

By

Amir Rouhani

******

Supervisor(s):

Dr. Seifeddine Jomaa

Associate Professor Alberto Viglione

Politecnico di Torino
2023

Declaration

I hereby declare that the contents and organization of this dissertation constitute my own original work and do not compromise in any way the rights of third parties, including those relating to the security of personal data.

Amir Rouhani

2023

* This dissertation is presented in partial fulfilment of the requirements for **master's degree** in the Graduate School of Politecnico di Torino.

I would like to dedicate this thesis to my loving family.

Acknowledgment

I would like to express my heartfelt gratitude to my supervisors, Dr. Seifeddine Jomaa of the Helmholtz Centre for Environmental Research - UFZ and Associate Professor Alberto Viglione of the Polytechnic University of Turin, for their unwavering support, guidance, and invaluable insights that have been instrumental in the successful completion of my master's thesis. Their tremendous expertise, ongoing drive, and outstanding mentorship have been incredibly motivating, and I consider myself extremely fortunate to have worked with them.

I'd also like to thank Associate Professor Marco D'Oria of the University of Parma and Professor J. Jaime Gómez-Hernández of the Polytechnic University of Valencia for their help and advice. Their experience, ideas, and helpful input have been important in developing my study work throughout, and I am genuinely thankful for their time and efforts.

Finally, I'd want to express my gratitude to my family for their constant support and encouragement during my studies. Thank you for being a part of my journey; I will always be grateful for your encouragement and support.

Abstract

Groundwater represents a strategic freshwater resource for multiple sectors, including drinking water, agriculture production, and ecosystem services. The Mediterranean Basin is a well-known water-scarce region that is increasingly relying on groundwater use, especially during drought periods. Many areas in the Mediterranean region are already facing water stress due to increasing demand and limited resources. Climate change is likely to exacerbate these issues, as it is expected to lead to more frequent and severe drought conditions in some areas as well as irregular rainfall in others. Due to the growing availability of data and computational processing capabilities nowadays, deep learning models are seeing an increase in popularity. In this study, we attempted to create 92 location-specific Convolutional Neural Network (CNN) models in wells spatially distributed over the Iberian Peninsula to estimate groundwater levels until the end of the century. Our models use monthly precipitation and temperature data as input variables. Specifically, we considered cumulative precipitation for 3, 6, 12, 18, 24, and 36 months to account for the recharge time lag between precipitation and groundwater changes. Once trained using historical precipitation and temperature records, the CNNs were applied to assess the influence of climate change on groundwater levels. For future climate projections, an ensemble of six combinations of distinct General Circulation Models (GCMs) and Regional Climate Models (RCMs) was considered under two Representative Concentration Pathways (RCPs): the RCP4.5 and RCP8.5. Our preliminary results revealed a more consistent decline in groundwater levels in the southwest region of the Iberian Peninsula under the RCP8.5 scenario, while a general more constant groundwater level under the RCP4.5 scenario has been detected towards the end of the century.

Keywords:

Groundwater level, climate change, deep learning, water scarcity, Iberian Peninsula, groundwater sustainability

Acronyms and abbreviations

AEM: Analytic Element Model ---------- 5
AI: Artificial Intelligence ----------XI, 1, 2, 8, 9, 10, 21, 37, 38, 56
ANN: Artificial Neural Network ---------- 6, 10, 11, 13, 38
ELM: Extreme Learning Machine----------11
ESD: Extreme Studentized Deviate ---------- 17, 41
FDM: Finit Difference Model ---------- 5
FEM: Finit Element Model ---------- 5
FNN: Feedforward Neural Network----------11
GCM: Global Climate Model ----------22
GPR: Gaussian Process Regression ----------11
GWL: Groundwater Level ---------- 7, 8, 9, 10, 11, 38, 39, 42
HP: Hyperparameter ---------- 13, 18
IPCC6: Intergovermental Panel on Climate Change Sixth Assessment Report --23
LSTM-LA: Long Short-Term Memory-Lion Algorithm ----------11
ML: Machine Learning---------- 10, 37
MLR: Multi Linear Regression ----------10
MM: Mathemetical Model----------10
NARX: Nonlinear Autoregressive Model with Exogenous Inputs11, 13, 50, 52, 53
NSE: Nash-Sutcliffe Efficiency ---------- XI, 18, 19
P: Precipitation---------- 11, 21, 44, 45, 47, 48, 50, 51, 54, 55, 57
R^2: Squared Pearson r---------- XI
RCM: Regional Climate Model----------22
RCP: Representative Concentration Pathway-IX, XI, XII, 6, 22, 23, 28, 30, 34, 37
RF: Random Forest ----------10
RMSE: Root Mean Square Error ---------- 11, 18
rRMSE: relative Root Mean Square Error ----------18
SVM: Support Vector Machine ----------10
T: Temperature ---------- 11, 21, 44, 47, 48, 50, 51, 52, 54, 56, 57
WTD: Water Table Depth ----------XI, XII, 18, 21, 27, 30, 32, 34, 35

Contents

List of Figures

List of Tables

Chapter 1

Introduction

Motivation

Climate change's influence on water supplies is a critical issue that demands quick response. Groundwater, the world's biggest freshwater reserve, is vital in delivering water to millions of people worldwide. The Iberian Peninsula is an excellent example of a place where groundwater is essential, particularly in arid and semi-arid areas. This region is also seeing increased climate change impacts, such as droughts and extreme weather events, which might have serious consequences for groundwater resources.

Machine learning (ML) and Artificial intelligence (AI) technologies have showed considerable promise in predicting and modelling complex systems, particularly groundwater, in recent years. A German research has previously shown that deep learning technology can successfully estimate groundwater levels in Germany using only weekly precipitation and temperature data as input. Nevertheless, the method's applicability to other locations is unknown.

As a result, the purpose of this thesis is to evaluate the use of deep learning technology in forecasting groundwater levels in the Iberian Peninsula. We will make slight changes to the approach to account for the time lag between groundwater system response and precipitation events. This study will help us understand the effects of climate change on groundwater resources in the Iberian Peninsula, as well as the possibilities of applying ML and AI technologies to model and predict groundwater systems.

This study is essential for policymakers and stakeholders because it gives vital insights into the effects of climate change on groundwater supplies, as well as the possibilities for adopting novel technology to mitigate these effects. The findings of this study can also be used to establish long-term water management policies for the region.

Importance of ground water

Groundwater is a nearly universal source of typically excellent freshwater. These properties encourage its broad growth, which may be scaled and localized to meet demand without the need for extensive infrastructure. Globally, ground water accounts for one-third of all fresh-water withdrawals, accounting for 36%, 42%, and 27% of water utilized for household, agricultural, and industrial purposes, respectively [1]. Water availability is a major economic and social priority for most Mediterranean nations since they share various characteristics such as similar water and land resources, agricultural expansion, demographic pressure paired with increased tourism, and, last but not least, a climatic shift moving from semiarid to arid conditions [2], [3]. Groundwater is the main source of water for irrigation in the Iberian Peninsula [4] and it is a critical resource for the agricultural sector in the Mediterranean region [5]. In addition to its importance as a source of freshwater, groundwater also plays a vital role in the environment as a major contributor to the baseflow of streams and rivers in the Mediterranean region, providing a vital source of water for ecosystems [6].

The Mediterranean basin has a limited supply of water, which is mostly supplied by mountain runoff [7]–[9]. These comprise 20-50% of total flow, although in semi-arid places such as the Mediterranean basin, runoff can contribute 50-90% [8], [10].

According to data from the Spanish Ministry of the Environment and Rural and Marine Areas, the Iberian Peninsula experiences a very irregular distribution of water resources due to its fluctuating precipitation, which ranges from less than 200 mm/year to more than 1,600 mm/year and even reaches 2,000 mm/year at times [11] Groundwater accounted for 32.2% of total water for residences and industrial purposes (excluding irrigation), municipal consumption, and other uses, according to statistics from the Spanish National Institute of Statistics [12]. This percentage ranges between 28.5% and 31.9%, according to the sources [13]. The disparity in this example is caused by the combination of survey-based data and subjective assessments. Groundwater contributes in the range of 17.5-29.5% of irrigation water, which accounts for 75% of total water usage in Spain.

Economic expansion is frequently accompanied by significant land-use changes and intensive human effects. Tourism has largely replaced forestry and agriculture in many Mediterranean nations, particularly along the coast. Population pressure has increased, causing issues with fresh water supplies and trash disposal

[14]. Groundwater resource extraction is vital and has grown even more so in recent years, particularly in coastal areas of dry and semi-arid countries. The influx of salty marine water puts the coastal aquifers in these areas under particular danger [15].

Climate change

There are several scientific mechanisms through which climate change can affect groundwater levels.

- One proposed mechanism is **evapotranspiration**, which is the combined loss of water to the atmosphere caused by soil evaporation and plant transpiration. As the Earth's temperature rises, so does the rate of evapotranspiration, resulting in a higher loss of water from the Earth's surface. This can lead to a drop in groundwater levels because water that would otherwise be available to recharge subsurface aquifers is lost through evaporation.
- Changes in **precipitation** patterns are another proposed way through which climate change might alter groundwater levels. The volume and distribution of precipitation (such as rain and snow) that falls may alter as the earth's temperature rises. There may be a rise in precipitation in some areas, which might lead to an increase in groundwater levels. In some areas, there may be a decrease in precipitation, which might lead to a drop in groundwater levels.

The scientific mechanisms by which climate change influences groundwater levels are complex and may differ based on the geographical region in question as well as the precise temperature and precipitation changes that are occurring. In general, climate change will result in drier conditions in many parts of the world, particularly in the western Mediterranean [16]. Iberia Peninsula is a hotspot of groundwater-impacted area by 40% of precipitation reduction [17].

Groundwater modelling

Groundwater modelling is critical because it enables us to understand and detect changes in the groundwater system, which is a critical resource for many human and environmental systems. Groundwater is utilized for a variety of reasons, including drinking water, irrigation, industrial activities, and many more. It also plays an important function in the health of ecosystems and wetlands. Groundwater modelling can assist us in making wise decisions about how to effectively manage

and conserve this vital resource by simulating changes in the water table and water quality. Groundwater modelling has various major applications:

- **Water resources management**: Groundwater modelling is used to understand the potential yield of wells and aquifers, predict future changes in the water table and water quality, and evaluate the impacts of different water management scenarios.
- **Contamination control**: Groundwater modelling may be used to mimic the movement of pollutants and other contaminants, assisting in the identification of probable sources of pollution and evaluating the effectiveness of various cleaning processes.
- **Environmental impact assessments**: Groundwater modelling can be used to evaluate the impacts of development projects, such as landfills, mining operations, and infrastructure projects, on the groundwater system.
- **Climate change impact**: Groundwater modelling can also be used to evaluate the impacts of climate change on the groundwater system, which may be affected by changes in precipitation patterns, temperature, and sea level.
- **Water supply**: Groundwater modelling can be used to predict changes in the water table, water quality and water recharge in order to plan water supply and manage water resources.
- **Hydrogeological Investigation**: To understand the behavior of the aquifers and aquitards, it is important to conduct a hydrogeological investigation, which requires the use of numerical models and analytical solutions.

There are several models that may be used to simulate and forecast groundwater activity. These models are classed depending on the model's complexity, the type of data utilized as input, and the unique characteristics of the groundwater system under study. Some examples of common groundwater models are:

1. **Analytic Element Models (AEM)**: These models reflect groundwater flow and transport processes using analytic functions. They are reasonably easy to use and may be applied to a wide range of groundwater systems, but their capacity to depict complicated groundwater systems is restricted [18]–[20]. Some examples are the Dupuit approximation [21], commonly used to simulate groundwater flow in unconfined aquifers, the Hantush model [22], which is used to simulate the flow of water in confined aquifers and the

superposition model [23] which is used to simulate the flow of water in an aquifer that has multiple layers with different hydraulic properties.

2. **Finite Difference Models (FDM)**: These models split the groundwater system into a grid of cells and solve for groundwater flow and transport inside each cell using finite difference equations. FDMs have a wide range of applications in groundwater systems, but they are restricted by the size of the grid and the precision of the finite difference approximations. Some examples are MODFLOW [24] which is a widely used FDM for simulating groundwater flow in three dimensions and FEFLOW [25] which is another popular FDM for groundwater modeling that is capable of simulating groundwater flow, solute transport, and heat transport in both saturated and unsaturated zones.
3. **Finite Element Models (FEM)**: These models, like the previous ones, split the groundwater system into a grid of cells, but they employ the finite element approach to solve for groundwater flow and transport inside each cell. Although FEMs are more precise than FDMs, they demand more computer resources and are more difficult to utilize. Some of the most popular FEMs are MODFLOW-2005 [26] with MT3DMS [27]. While MODFLOW is primarily a finite-difference model, it also has a finite-element option that can be used in conjunction with MT3DMS for solute transport modelling and HYDRUS [28], which is a finite-element model specifically designed for simulating water flow, heat transport, and solute transport in unsaturated porous media.
4. **Statistical Models**: These models fit a model to observed groundwater data using statistical approaches. They are frequently utilized when data is scarce and are useful for establishing probabilistic forecasts regarding future groundwater conditions. The most common statistical model is multiple regression analysis which relates two or more independent variables to a dependent variable.
5. **Artificial Neural Network Models (ANN)**: These models fit a model to observe groundwater data using artificial neural networks. They are comparable to statistical models in that they can make more accurate predictions and handle vast volumes of data.
6. **Hybrid Models**: These models incorporate aspects from other model types, such as AEMs, FDMs, and ANNs, to capitalize on the benefits of each. Complex groundwater systems are frequently simulated using hybrid models.

Our study

This thesis project, which was inspired by a German paper [29], investigates how climate change will directly influence groundwater resources in the Iberian Peninsula during the twenty-first century by applying a deep learning groundwater level prediction approach based on convolutional neural networks to 92 sites well distributed across the region to assess groundwater level development under various RCP scenarios.

Objectives

The main aim of this study is to test the capability of deep learning methods to assess the impact of climate change on groundwater levels in the Iberian Peninsula. Specifically, the objectives of this work are to (i) select the groundwater systems that are mainly controlled by climate forcing, (ii) explore the best explanatory variables of cumulative precipitation, reflecting different groundwater recharge time lags (3, 6, 9, 12, 18, 24 and 36 months), that explain better the groundwater level changes, and (iii) evaluate the impact of climate change on groundwater levels under the RCPs 4.5 and 8.5 scenarios and considering three time periods (near [2021-2040], mid [2041-2060] and long term [2081-2100]).

Chapter 2

Literature review

Groundwater modelling

Being one of the world's most valuable and essential sources of water, groundwater resources play a direct and crucial role in many aspects of human existence, including agriculture, industrial development, and potable water supply [30], [31]. Furthermore, the evident consequences of groundwater resources on the environment and society cannot be overstated. The groundwater level is a clear and straightforward indicator of groundwater availability and accessibility. A good knowledge of GWL's history, current, and future conditions may give policymakers and practitioners in the water sector with greater insight and perception to establish strategies for water resource planning and management, ensuring sustainable socioeconomic development [30]. Yet, GWL is an integrated response to various climatic, topographical, and hydrogeological elements and their interconnections, making GWL simulation a difficult undertaking [32], [33].

The modelling of groundwater systems is thought to have started in the early 20th century, with the work of people like Karl von Terzaghi, who is considered the father of soil mechanics, and his student Ralph B. Peck. They were among the first to use mathematical models to study the behaviour of groundwater and its interactions with soil and other subsurface materials. However, the first documented use of mathematical modelling of groundwater systems could be traced back to the late 19th century when the first analytical solutions for confined aquifers were proposed by French engineer H.E. Dupuit [34].

There are many types of models used to simulate and predict the behaviour of groundwater systems, and they can be broadly categorized into two groups: analytical and numerical models.

Analytical models are based on mathematical equations that can be solved analytically or with simple mathematical techniques, to produce a closed-form solution. Examples of analytical models include the Dupuit-Forchheimer equation

[35], Theis equation [36], and Hantush-Jacob equation [22], [37]. These models are typically used to simulate the behaviour of confined or semi-confined aquifers and are relatively simple to use and understand.

Numerical models are based on mathematical equations that are solved using numerical methods, such as the finite element or finite difference method. These models are generally more complex than analytical models, but they can be used to simulate a wide range of groundwater flow and transport processes. Some examples of numerical models are MODFLOW [24], FEFLOW [25], MODPATH [38], MODFLOW-NWT [39], and MT3DMS [40]. These models are widely used by researchers, engineers, and water resource managers to simulate and predict the behaviour of groundwater systems in a variety of settings. Both types of models are used by researchers, engineers and water resource managers, but numerical models are more widely used in current practices. Although these classical models are durable and dependable, the precision and accuracy of numerical models are limited by various variables, including their reliance on vast quantities of data relating to aquifer characteristics, porous media geology, and basement topography [41]. Furthermore, accurately demarcating domain boundaries, establishing an optimal grid size for solving the corresponding differential equations, and calibrating/validating the executed model have all contributed to numerical modelling being a demanding and sophisticated undertaking [42].

Machine learning history

In recent years, there has been an increase in the application of machine learning in groundwater-level modelling. Several factors are driving this trend, including the availability of massive databases of groundwater measurements that can be used to train machine learning algorithms. Growing processing capacity and the availability of tools for applying machine learning algorithms have made it simpler for academics and practitioners to use these approaches to groundwater modelling also the awareness that, as compared to traditional modelling methodologies, machine learning may give more accurate and complex models of groundwater dynamics but when compared to physically based and numerical approaches, the ability of Artificial Intelligence (AI) models to simulate and predict groundwater level (GWL) without requiring a deep and thorough understanding of the underlying topographic and hydro-geophysical factors makes them desirable methodologies [43]. **Figure 1** depicts the number of publications each year in the field of groundwater modelling using various AI algorithms from 2000 to 2022. Data was gathered from the Web of Science database using the search prompt:

- Topic: groundwater
- Title: groundwater AND ("artificial intelligence" OR "machine learning" OR "neural network" OR "deep learning")
- Abstract: modeling OR modelling

In total 435 publications were found, which we tried to display by year of publication, and it clearly demonstrates an exponential increase in the number of published papers, particularly since 2020.

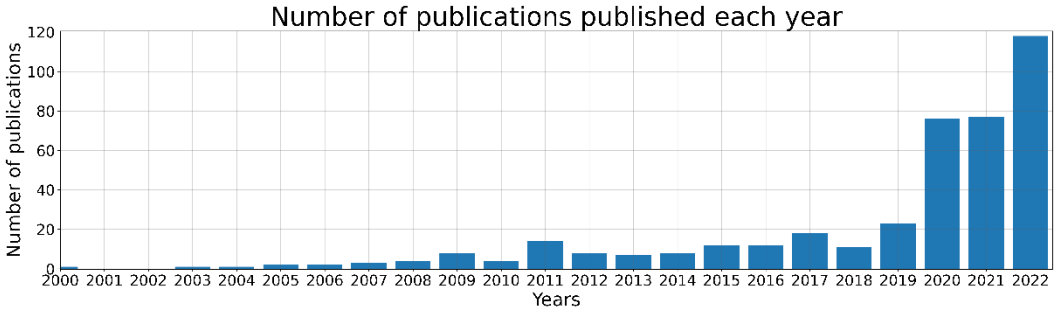

Figure 1. Arithmetical conceptualization of growth observed in groundwater research using AI based model during 2000-2022.

Artificial intelligence for GW modelling

Although classical models are durable and dependable, the precision and accuracy of numerical models are limited by various variables, including their reliance on vast quantities of data relating to aquifer characteristics, porous media geology, and basement topography [44]. Moreover, accurately demarcating domain boundaries, establishing an optimal grid size for solving the corresponding differential equations, and calibrating/validating the executed model have all contributed to numerical modelling being a demanding and sophisticated undertaking. Artificial intelligence (AI) models have been widely employed in the last two decades to address the shortcomings of traditional numerical models for GWL simulation [42].

In recent years, the use of data-driven models, including machine learning, has grown in popularity in groundwater modelling [42]. Several factors are driving this trend, including rising computational power, the availability of big datasets, and developments in monitoring devices that enable real-time, precise data collecting. Groundwater hydrology has benefited from machine learning and data mining applications [45]. When compared to physically based and numerical approaches,

the ability of AI models to simulate and predict GWL without requiring deep and complete understanding of the underlying topographic and hydro-geophysical factors makes them desirable methodologies [46]. Despite all of ML's benefits, the constant evolution of approaches makes it difficult for academics to evaluate the most successful methodology and its effectiveness on GWL prediction [47]. Statistically in recent years, it has been revealed that mathematical models (MM) techniques for predicting groundwater level fluctuations have been utilized less frequently. Machine learning has superseded mathematical models, and the random forest (RF) method is the most often used technique for forecasting groundwater level changes [47].

Commonly used machine learning techniques

Researchers have used a variety of machine learning (ML) models to predict changes in groundwater level (GWL), including Yang et al. [48], who used a hybrid ML model, Sahoo et al. [49], who used an ensemble modelling framework based on spectral analysis, machine learning, and uncertainty analysis, Chang et al. [50], who used two ANN models, Gaffoor et al. [51], who used random forest (RF), and Jyolsna et al. [52], who used two commonly used machine learning models: multi-linear regression (MLR) and random forest (RF). The most frequent machine learning models used for constructing inferential models for water quality evaluation, according to relevant research published between 2001 and 2021, are artificial neural networks, random forest, and multiple linear regression [53]. Although some studies used artificial neural networks (ANN) [54], support vector machine (SVM) [55], and random forest (RF) [56] methods, others [57] used support vector machine, generalized regression neural network, convolutional neural network, long short-term memory (LSTM), and gated recurrent network to simulate GWL changes. For example, in ref. [52], multi-linear regression (MLR) and random forest (RF) approaches were used.

Deep learning models are made up of three layers: an input layer, hidden layers, and an output layer, with a neural network used to map information into the output layer. CNN and LSTM are the most often used deep learning algorithms in hydrological research [58]. In general, the literature reports on three key categories of deep learning applications in groundwater: (1) comparison of the performance of different deep learning algorithms; (2) filling missing data values; and (3) enhancement of the simulation framework. Kumar et al. [59] compared deep learning, Extreme Learning Machine (ELM), and Gaussian Process Regression (GPR) to estimate groundwater level in the Konan basin, Japan, using precipitation

(P), river stage, temperature (T), recharge, and groundwater level as input data. Supreetha et al.[60] did similar research in the Udipi area of Karnataka, India, and discovered that the Long Short-term Memory-Lion Algorithm (LSTM-LA) outperformed the LSTM and Feedforward Neural Network (FNN) in groundwater level prediction.

Vu et al. [61] assessed the capacity of an LSTM to forecast future GWL changes in northern Normandy, Italy, by filling in the 50-year GWL data at 31 piezometers. They concluded that using deep learning to reconstruct GWL fluctuations is feasible, with correlation coefficient and RMSE values of 0.64-0.99 and 0.07-1.08 m, respectively. Sun et al. (2019) [62] used deep learning and hydrological models to fuse GRACE satellite data with NOAH-aland surface model established by NASA to enhance groundwater storage prediction in India. The deep convolution neural network (CNN) model was used to learn the spatio-temporal discrepancy in GRACE and NOAH groundwater trends. According to their findings, CNN enhanced the GRACE-NOAH match and successfully filled data gaps between GRACE missions.

In recent years, artificial neural network (ANN) methods have proven useful in forecasting groundwater levels [63]–[68], even when utilizing a highly transferrable approach with just climate input data. In a previous study [68], it has been demonstrated that 1D-convolutional neural networks (CNNs) are a good choice for groundwater level simulation because they outperform even long short-term memory (LSTM) models in terms of accuracy and calculation speed, and they demonstrated significantly higher flexibility and modelling stability when compared to NARX models (nonlinear autoregressive models with exogenous inputs). As a result, they are an accurate, quick, and dependable method of choice for this investigation.

Machine Learning for Predicting Future

Machine learning algorithms have traditionally been used to estimate groundwater levels based on current observations and historical data. Yet, as people become more aware of the effects of climate change on groundwater supplies, there is a rising interest in utilizing machine learning models to forecast future groundwater levels under various climate change scenarios. Recent research has demonstrated that machine learning approaches, such as deep learning models, can capture the intricate interactions between climatic factors and groundwater levels and produce solid predictions of future groundwater levels. These models may

account for a variety of parameters such as temperature, precipitation, land use, and human activities, and they can give useful insight into the possible effects of climate change on groundwater supplies. While there are still challenges and limitations to using machine learning models to predict future groundwater levels, such as data availability and model uncertainties, these models have the potential to improve our understanding of the effects of climate change on groundwater resources in the future and support effective groundwater management and planning.

Chapter 3

Methodology and data

Convolutional neural networks

Artificial neural network (ANN) techniques have shown successful in forecasting groundwater levels in recent years [69]–[74], even when utilizing a highly transferrable approach with just climatic input factors. 1D-convolutional neural networks (CNNs) are an excellent choice for groundwater level simulation because they outperform even long short-term memory (LSTM) models in terms of accuracy and calculation speed, and they demonstrated significantly higher flexibility and modelling stability when compared to NARX models (nonlinear autoregressive models with exogenous inputs) [74]. As a result, they are an accurate, quick, and dependable method of choice for this investigation [29].

In this study, we use a 1D-CNN approach to build 92 site-specific models that have been selected through a multi-step procedure and are relatively well distributed across the Iberian Peninsula and are capable of predicting monthly groundwater levels with high accuracy using precipitation in monthly and accumulated 3, 6, 12, 18, 24, and 36 months as inputs in the past. CNNs are frequently employed for image processing and classification applications, but they also perform well with sequential data, such as groundwater level time series. The CNNs utilized in this work include a 1-D convolutional layer with a fixed kernel size (three) and an optimal number of filters, followed by a Max-Pooling layer and a Monte-Carlo dropout layer with a fixed dropout of 50% to prevent overfitting. This high dropout rate necessitates highly strong training for the model. Following that is a thick layer with an optimal number of neurons, followed by a single output neuron. The Adam optimizer was used for a maximum of 100 training epochs with an initial learning rate of 0.001 and gradient clipping was utilized to prevent exploding gradients. Another regularization strategy used to prevent the model from overfitting the training data was early halting with a patience of 15 epochs. Bayesian optimization was used to tune several model hyperparameters (HP) [75]: training batch size (16-256); input sequence length (1-52 months); the number of filters in

the 1D-Conv layer (1-256); and the size of the first dense layer (1–256). All models were built with Python 3.8 [76], the TensorFlow deep-learning framework [77], and its Keras API [78]. NumPy [79], Pandas [80], [81], Scikit-Learn [82], BayesOpt [83], Matplotlib [84], UnumPy [85], PyAstronomy [86] and SHAP [87] libraries were also utilized. [29].

Historical data

We utilized a grided dataset of daily precipitation and temperature over Iberia [88], [89] for historical climate data. Precipitation acts as a proxy for groundwater recharge, while temperature serves as a proxy for evapotranspiration. Furthermore, temperature has a distinct yearly cycle, which supplies the models with vital information on seasonality. This dataset includes a new observational gridded dataset (referred to as Iberia01) for daily precipitation and temperatures measured at 0.1° regular (and 0.11° CORDEX-compliant rotating) resolutions throughout the Iberian Peninsula from 1971 to 2015. To eliminate uncertainty caused by grid cell size, the mean of 3 × 3 cells around the cell containing the appropriate well was used for each location.

In Spain, we used data provided by the Ministry of Ecological Transition and Demographic Challenge, which hosts the Piezometric Monitoring Network [90], [91], which was downloaded with a web scraping code done in early 2020, and in Portugal, it is run by the National System of Hydrologic Information [92], [93] as part of their monitoring databases, which were downloaded by hand in early 2020. These were monthly minimum, maximum, and average water table depths (WTD) from ground surface measurements, as well as the date of measurement. Our raw data was compiled from 940 wells in Portugal and 2889 wells in Spain, totalling 3829 wells. **Figure 2** depicts the raw data distributions over the Iberian Peninsula along with their geological formations.

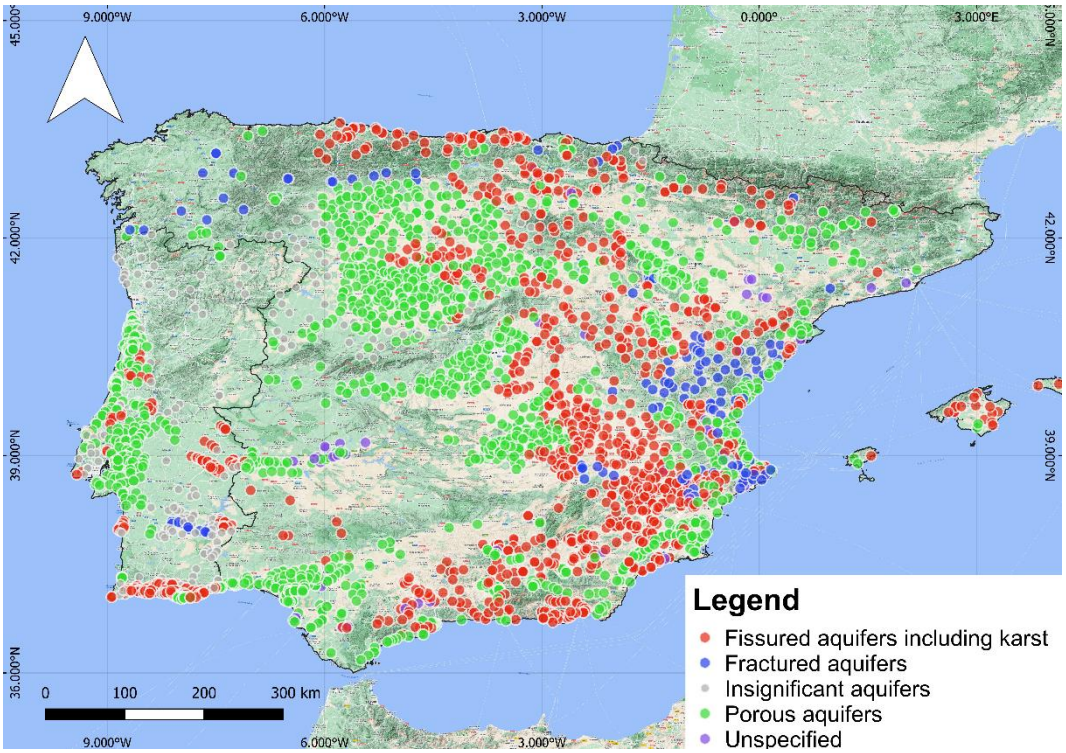

Figure 2. Distribution of the raw data in whole Iberian Peninsula.

Preprocessing

In machine learning projects, data preprocessing is one of the most important stages in order to understand what kind of data you are dealing with and how the data quality is because you are usually dealing with a large number of data sets, and in our case, the total of 3829 datasets are a relatively large number of data sets and we have no idea about the duration, start, end, frequency of measurements, and so on.

Cleaning and filtering data

We decided to remove Nan and zero values from all data sets during the preprocessing stage because Nan values were related to unsuccessful or no measurements and zero values were also related to a mistaken or incorrect measurement. After removing these values, we had 2872 wells in Spain and 936 wells in Portugal, so 21 wells were eliminated due to the lack of a single valid measurement. We are confident that the rest of the data set contains measurements.

We used a bottom-up strategy for our analysis, as opposed to the inspired paper [29], which chose especially unconfined, shallow aquifers that are most likely to be subject to direct climate change effects. As we have added cumulative precipitations to account for the lag between groundwater system response and precipitation, we have decided to feed all datasets that we have to the model and let the model decide which features are most related to the system. With this methodology, we hope to find some deeper groundwater systems than the main paper [29], which only focused on the shallow layer. To that end, because deep learning models require large data sets to work, we chose to filter the data sets before feeding them into the model. As a result, we select them depending on data availability.

Furthermore, we employed two parameters. The first was the number of measurements, while the second was the percentage of missing data. Because our measures vary from one in each month to every two months, and so on. So, to increase the number of measurements between the first and last measurements, we utilize this parameter to construct a subset of the data set. The thresholds we choose here are for the number of measurements to be equal or greater than 120 measurements and for missing values percentage to be equal or less than 50%, and the combination of these two conditions resulted in 1205 wells, which we then sort based on the number of measurements, starting with the ones with the most measurements and working our way down.

Outlier removal

An outlier is an observation that deviates from the rest of the data. Outlier approaches are classified into two types: test discordance methods and labeling methods. The majority of outlier detection systems consider extreme value to be an outlier. There is no need to employ a statistical table in some circumstances of outlier identification methods [94]. To identify the numerous ways in which outliers may originate. It is necessary to examine them in greater depth. Various sources of variability might be encountered when taking observations. We can tell three of them apart [95].

- **Inherent variability**: This is an indication of how observations fluctuate inherently across the population; such variance is a natural aspect of the population and is uncontrolled. Men's height measurements, for example, will represent the level of variability inherent in that demographic.
- **Measurement error**: We frequently need to conduct measurements on individuals of a population under investigation. Inadequacies in the

measurement device add another degree of unpredictability to the underlying component. The rounding of data, or errors in recording, compound the measurement error: they are a component of it. This sort of unpredictability can be managed to some extent.

- **Execution error**: Another cause of variation occurs from the inadequate collecting of our data. We may mistakenly choose a biased sample or include individuals who are not actually representative of the group we want to study. Again, prudent procedures may help to limit such fluctuation.

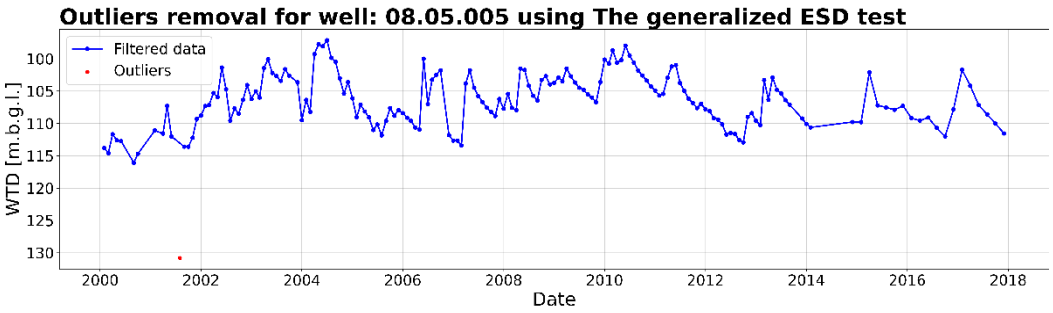

Figure 3 Generalized ESM outlier removal result for well 08.05.005.

In this work, we do not analyse the kind and source of outliers, but rather strive to exclude them from the data so that we may train our models with higher-quality data. Considering most common outlier removal methodologies Hampel, Quartile, and generalized (Extreme Studentized Deviate) ESD surpass Grubbs and Dixon among the most prevalent and advanced outlier detection and removal algorithms [94]. The main restriction of the Grubbs test is that the suspected number of outliers, k, must be precisely defined. If k is not provided appropriately, the results of these tests may be distorted. The generalized ESD test [96], on the other hand, just requires an upper bound for the suspected number of outliers to be stated [97]. We chose the default value of 10 for the maximum number of outliers provided by the PyAstronomy [86] python package. Figure 3 shows the result of outlier removal for a random well where the approach discovered and deleted one outlier.

It is also worth noting that in this study, we decided not to do any interpolation on the input data because the number of missing values for a substantial number of piezometers was very high and occurred in the center of the time series. For example, a 2-year period of missing values in the middle of a 10- or 12-year period of timeseries data, as was the case for all surrounding wells, and secondly, because we are using the bottom-up methodology and feeding all of our data to the model, we decided not to use any interpolation to increase the reliability of the results.

Models training and selection

After completing the preprocessing stage, we are now ready to begin the model's first step, which is the hyperparameter acquisition and optimization. To that purpose, we employed monthly water table depth (WTD) time series data of varying lengths, as well as meteorological data sets, as explanatory variables from 1974 to 2015. Because the first 3 years of data were removed to generate the cumulative precipitation data.

The model divides each time series into four segments to identify the optimal model configuration: training set, validation set, optimization set, and test set. The test set always utilizes the four-year period from 2012 to 2016, and for a few locations where the time series terminated sooner, the four-year test set period is shifted correspondingly. The first 80% of the remaining time series before 2012 were utilized for training, the next 20% for early stopping (validation set), and the final 10% for testing during HP optimization (optimization set), each employing 10% of the remaining time series [29]. A maximum optimization step number of 150 was employed for each model, otherwise, it stops after 15 steps without improvement after a minimum of 60 steps was achieved. To lessen reliance on the random number generator seed, it scales the data to [-1,1] and uses an ensemble of 10 pseudo-randomly initialized models. It uses Monte-Carlo dropout during simulation for each of the ten ensemble members to estimate model uncertainty from 100 realizations. The 95% confidence interval was then calculated from these 100 realizations using 1.96 times the standard deviation of the resultant distribution for each time step. To assess simulation accuracy, the model computes various measures, including NSE, squared Pearson r (R^2), absolute and relative root mean squared error (RMSE/rRMSE), and absolute and relative Bias (Bias/rBias) in **Figure 4**. [29].

At the end of this step, we had the results for 1103 wells, and 102 wells were eliminated during this stage of hyperparameter acquisition. The reason for this could be primarily a lack of data because the eliminated datasets were mostly at the bottom of the list, where we had ordered them based on the number of measurements. After we had all of the results for the 1103 model, we chose to filter them using the R^2 and NSE indicators to focus on the models that are more accurate. To that end, we opted to filter them based on NSE greater or equal to 0 and R^2 greater or equal to 0.5, which resulted in 170 models clearing the barrier. **Figure 5** attempts to depict the region on which we decided to focus the rest of the investigation and **Figure 6** depicts the distribution of these 170 wells around the

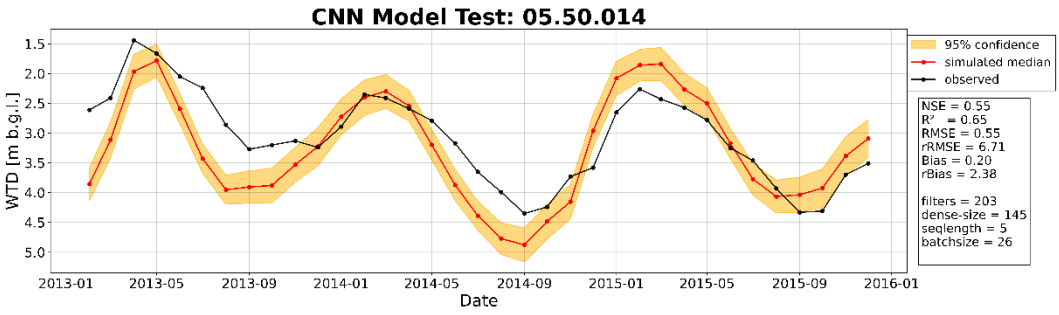

Figure 4. Hyperparameter and test results for well 05.50.014.

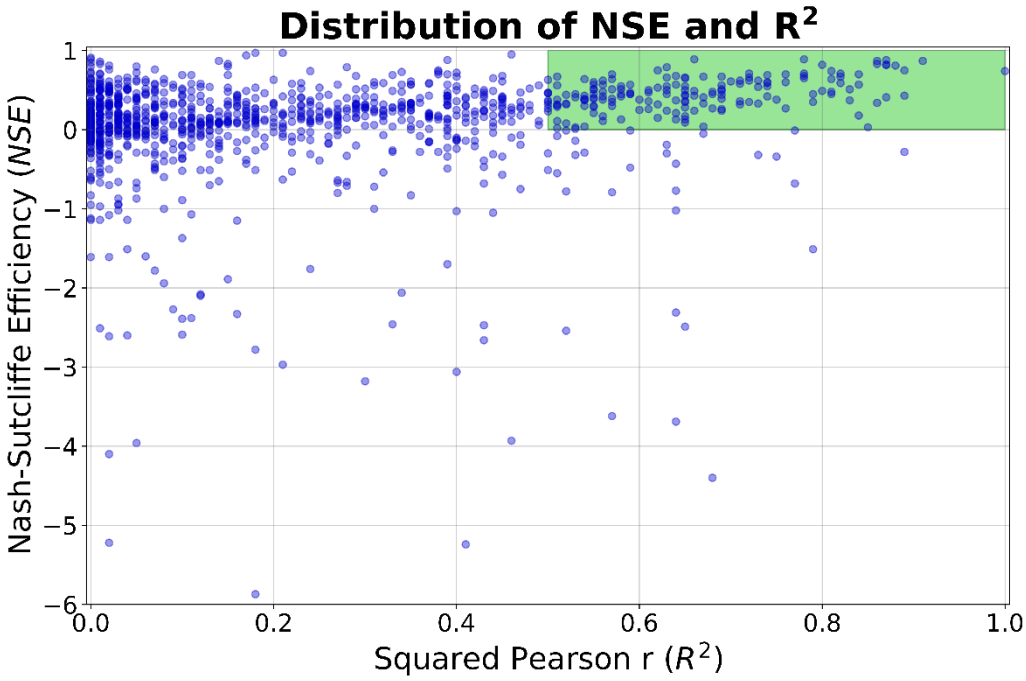

Figure 5. scatter plot of NSE on Y axes and R^2 in X axes of all models and the blue rectangle shows the selected models.

region, with the filtered wells primarily located towards the coast, where there are shallower aquifer systems. The only region with no wells is the north-west section of the Iberian Peninsula, which may be owing to a lack of data availability in this area. Because we can see from the distribution of all wells in **Figure 2** that there is no data from this region as well. The geological formation of the wells described as colors is also shown in **Figure 6**, and we can see that the majority of these wells are porous aquifers, which have been followed by fissured aquifers, including karst.

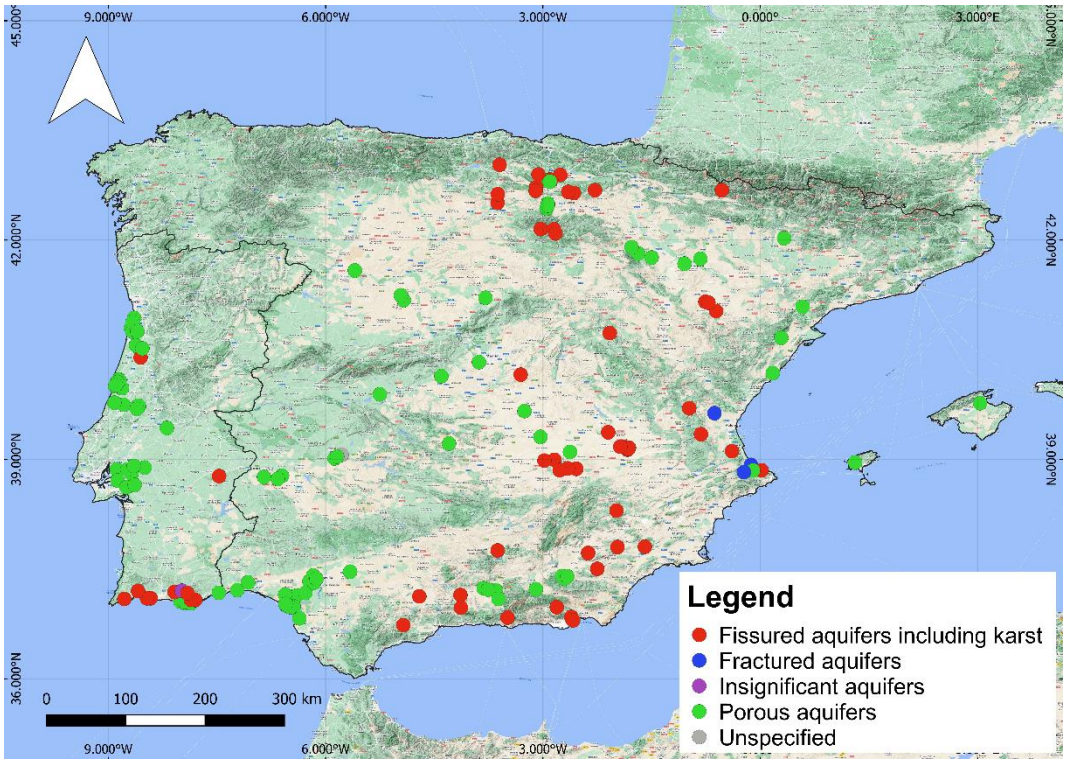

Figure 6. Distribution of the 170 filtered wells based on the NSE and R^2 in the region with the color legend indication geological formation of the aquifer system.

An idealized test is created to push the model well beyond the long-term range of probable inputs as the next stage to evaluate if the CNN model is capable of producing physically reasonable results even when inputs are not within the range of the training data. The model was run with quadruple precipitation and a 5-degree Celsius temperature rise over the training set [98] (**Figure 8**).

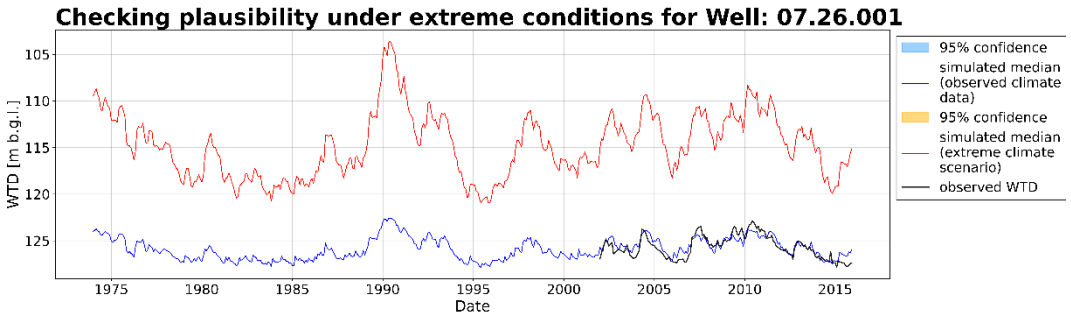

Figure 8. Model output under an artificial extreme climate scenario in the past (1974 - 2015).

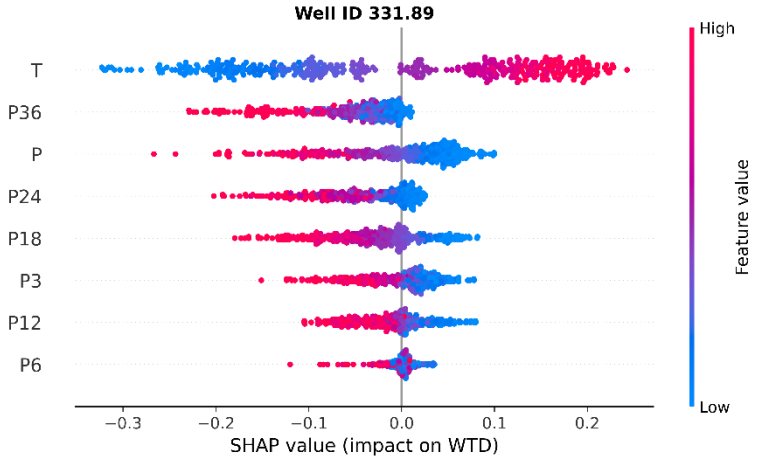

Figure 7. SHAP Summary plot.

We also used an explainable AI technique to see if the models trained appropriately based on our conceptual understanding of hydrogeological processes. We produced SHAP values to describe the effect (sign and intensity) of each input feature value on the model output in **Figure 7**. In general, our models demonstrated that the link between input and output was plausible. High precipitation inputs, for example (P, red), cause low or negative SHAP values and hence have a large negative effect on the model output, which conforms to our fundamental knowledge of the influence of recharge, which leads to increased groundwater level. Low or no precipitation (P, blue) has a very minor beneficial impact on WTD, but high-temperature inputs (T, red) have a significant positive influence on the model result, implying reduced WTD. Again, this correlates to our basic knowledge of the regulating mechanisms, where high temperatures often result in high evapotranspiration, which results in decreased recharging or, in some situations, direct groundwater evaporation (**Figure 7**).

Prediction data and RCP scenarios

We chose just two Representative Concentration Pathways (RCPs) for future forecasts.

- **RCP4.5**: is a scenario in which emissions peak in the mid-century [2041-2060] and then fall, resulting in moderate warming.
- **RCP8.5**: in which emissions continue to climb throughout the century, culminating in extremely high levels of warming.

We also employed an ensemble of 8 Euro-Cordex GCM-RCM combinations which are reported in Table 1 with the same resolution as historical period. RCM stands for Regional Climate Model, which is a type of climate model that is used to simulate the climate at a regional scale. It is typically used to simulate the climate of a specific area, such as a country or continent, and can take into account the local topography, land use, and other factors that can affect the climate.

GCM stands for Global Climate Model, which is a type of climate model that is used to simulate the climate at a global scale. It considers the interactions between the atmosphere, oceans, land surface, and cryosphere (ice and snow) to simulate the global climate.

Both RCM and GCM are used to forecast future climate because they each have their own strengths and limitations. GCMs are able to simulate the large-scale patterns of climate, such as the circulation of the atmosphere and oceans, but they have lower resolution and may not accurately simulate the climate at a regional level. RCMs, on the other hand, have higher resolution and can simulate the climate at a regional level more accurately, but they are limited in their ability to simulate the large-scale patterns of climate.

By using a combination of RCM and GCM, scientists can take advantage of the strengths of each model to produce more accurate and reliable projections of future climate. The GCM is used to provide the large-scale climate patterns and boundary conditions, while the RCM is used to simulate the climate at a regional level with higher resolution. This approach allows for a more detailed understanding of how the climate is expected to change in specific regions and can help inform decision-making related to climate adaptation and mitigation.

The data begins in January 1976 and continues through December 2100. Because this time was used to bias-correct the climate model data, the data from

1976 to 2005 should reflect the average features of the historical data, but the data from 2006 to 2100 are forecasts based on the RCP8.5 and 4.5 scenarios. To decrease uncertainty caused by grid cell size, we used the mean of 3 × 3 cells around the cell containing the corresponding well as input for the simulations, as we did for the historical era for each location.

Table 1. Climate projections overview for both RCP scenarios.

Abbrev	Projections
M1	'CNRM_CERFACS_CNRM_CM5_CCLM4_8_17'
M2	'DMI_HIRHAM5_NorESM1-M'
M3	'ICHEC_EC_EARTH_HIRHAM5'
M4	'IPSL-INERIS_WRF381P_IPSL-CM5A-MR'
M5	'KNMI_CNRM-CM5'
M6	'MPI_M_MPI_ESM_LR_RCA4'
M7	'ICHEC-EC-EARTH_RACMO22E'
M8	'IPSL_IPSL_CM5A_MR_RCA4'

We utilized the IPCC AR6 suggested future periods for near-term (2021-2040), mid-term (2041-2060), and long-term (2081–2100). We do not have data for the historical period specified in AR6 of the IPCC from 1850 to 1900. As a result, we picked the years (1986 – 2005) as our reference period. We end in 2005 since the prediction period for the climate models we employ begins in 2006.

Visual filtering of the models

In this study, we decided not to rely just on statistical indicators to choose the optimal CNN model but rather to adopt a hybrid strategy in which a mixture of several indicators will provide us with the best and most dependable models to use for the projection stage.

Our objective was to analyze all of the results together in order to determine if everything works well together or not and to be certain about the models and projection outcomes. Given that the purpose of this study is not to predict the exact value of groundwater table depth in a specific period in the future, but rather to determine whether or not there is a trend for future circumstances. To that purpose, we plotted all of the outcomes for each well on one page next to each other and checked them one by one to determine if the model performs well for all 170 filtered wells. Test results, simulated results for the historical era and extreme conditions scenario, SHAP values, simulation results for one random future model scenario, and well location with corresponding groundwater body name were utilized for this stage. Appendix 1 contains the results of the HP optimization, extreme conditions, and SHAP summery map for all 92 wells.

Well 04.04.008 is an example of a well that was eliminated from the subset because the test results, simulation results for the historical period, and extreme scenario were all within acceptable ranges, but the SHAP values were not showing any sensible results because the model had responded for the different parameters in an unacceptable manner, and the future projections were unsatisfactory, so this model was eliminated in this step (**Figure 9**).

Uncertainty

Uncertainties in a CNN machine learning model can arise from a variety of factors, including poor data quality, poor model design, poor hyperparameter optimization, poor model generalization and poor model interpretation. A thorough examination of these sources of uncertainty can help to improve the model's performance and reliability.

Climate data quality varies depending on the source and processing technique, resulting in uncertainty in model inputs. To mitigate these uncertainties, thorough data preparation and quality control are required. In our case, we attempted to use a reliable data source first, and then, during the extraction of temperature and precipitation data for each well location, instead of using data only related to the closest well, we used the mean of the 3 by 3 cells around the closest grid point, plus for groundwater table depth data, we used a very specific method of Generalized ESM method, which was chosen based on the superiority of the given results in comparison to other methods Finally, in order to limit uncertainty, we did not use any interpolation techniques for missing measurements and worked only with in-situ data for WTD.

The architecture of a CNN model can impact the model's performance and accuracy, resulting in uncertainty in predictions. As a result, model architecture improvement and comparison can assist in reducing these uncertainties. The hyperparameter optimization, such as learning rate and batch size, can impact model performance and contribute to uncertainty in predictions. As a result, a systematic hyperparameter tuning procedure can aid in reducing these uncertainties. To that purpose, we used Bayesian optimization to optimize hyperparameters. This method uses a probabilistic model to represent the link between machine learning model performance and hyperparameters. Using a utility function that balances exploration and exploitation, the approach picks new hyperparameter combinations to assess. The benefits of Bayesian optimization include the fact that it requires less evaluations than other approaches, making it suitable for costly models, and its universal application to any machine learning model without the need for domain expertise [99].We utilized a maximum optimization step number of 150 for each model or stopped after 15 steps without improvement if a minimum of 60 steps was attained [29].

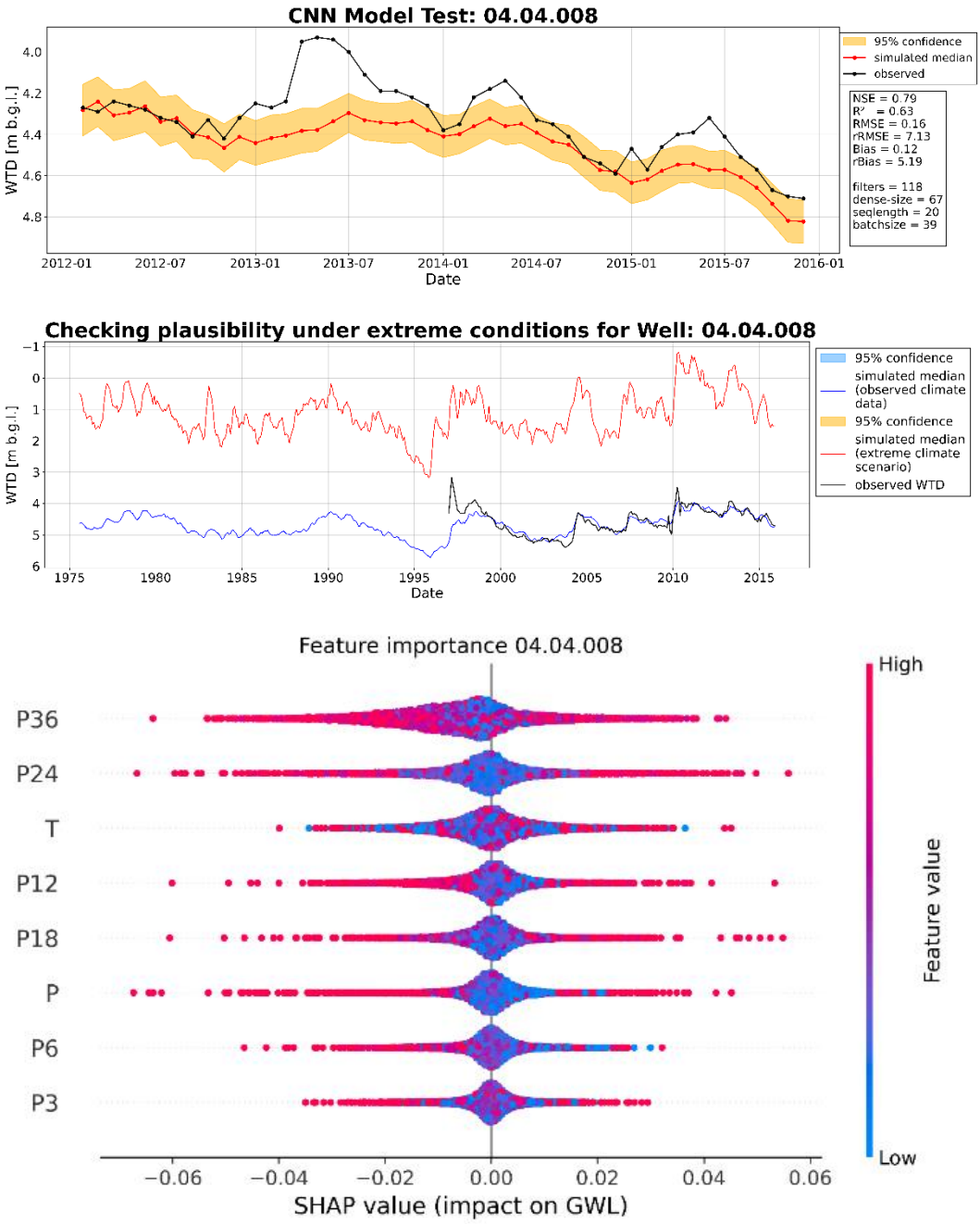

Figure 9. test result (up), simulation results for historical and extreme scenario (middle) and SHAP summery plot (bottom) for visual filtering step.

Overfitting can also occur in CNN models, resulting in poor generalization performance and uncertainty in predictions. As a result, approaches such as dropout and data augmentation can assist enhance the generalization performance of the model and minimize uncertainty. To lessen reliance on the random number generator seed, we scaled the data to [-1,1] and employed an ensemble of 10

pseudo-randomly started models. We used a Monte-Carlo dropout layer for each of the 10 ensemble members, with a fixed dropout of 50% to prevent the model from overfitting. This high dropout rate compels the model to undertake highly robust training and to estimate model uncertainty from 100 realizations each during simulation. Using 1.96 times the standard deviation of the resultant distribution for each time step, we calculated the 95% confidence interval from these 100 realizations [29].

Because of their complicated structure, CNN models can be difficult to interpret, resulting in uncertainty in predictions. As a result, tools such as visualization of the learnt features and attribution methods can aid in the interpretation of the model's predictions and minimize uncertainty. We computed SHAP values to explain the effect (sign and intensity) of each input feature value on model output, however we only utilized them to exclude models that were trained improperly in terms of our conceptual knowledge of hydrogeological processes.

When it comes to future predictions, the magnitude of uncertainty raised by future scenarios and models is too great when compared to those raised by models and data, and the only tool we have to consider them is to first consider different models that are combinations of different GCMs and RCMs to cover as much uncertainty as we can, and here we tried to consider 8 different models, and in the section of RCP scenarios, we decided to consider RCP4.5 as the best case scenario because the likelihood of the RCP2.6 scenario is determined by a number of factors, including the level of global collaboration and governmental action to reduce greenhouse gas emissions. However, it is worth highlighting that the RCP2.6 scenario indicates a low emissions trajectory that necessitates quick and strong action to restrict warming to less than 2°C over pre-industrial levels. It is hardly a business-as-usual situation and attaining it will need a fundamental overhaul of our energy infrastructure as well as considerable measures to cut emissions from other sectors. RCP8.5, on the other hand, predicts a future world with high levels of greenhouse gas emissions. It is also known as the "business-as-usual" scenario because it anticipates that global emissions would continue to climb throughout the twenty-first century as a result of rising energy consumption, population expansion, and limited attempts to reduce emissions.

Chapter 4

Results

The major purpose of this study was to determine the influence of climate change on WTD in the Iberian Peninsula, thus we trained 92 site-specific models based on various factors and methods described in Chapter 3. Taking into account the two RCP scenarios and the 8 distinct models for each model and location, we obtain 16 possible projection outcomes (8 for each RCP scenario) for each well, for a total of 1472 results for all 92 wells.

Figure 10 depicts the projected results for one random well as a heatmap from 2020 to the end of 2100. This graphic allows us to see all of the models and situations at once. The first row depicts the RCP4.5 scenario, where we can see that, with the exception of M2 and M6, the reduced greenhouse gas emissions of the RCP4.5 scenario translate to a distinctly reduced impact on water table depth development, which we can see as more blue and less red colors specifically in the long term period [2081-2100], but in M2 and M6, we can see more intense reds and less blues, which translate to higher WTD and depletion of groundwater levels.

Looking at the second row of **Figure 10**, we can see the findings for RCP8.5, where the negative influence of climate on water table depths is more apparent, and this is valid for all models when compared to RCP4.5. The shifts begin in the mid-term period [2041-2060] and intensify as we approach the long-term period [2081-2100]. When we evaluate different models, we can observe that the M2 model

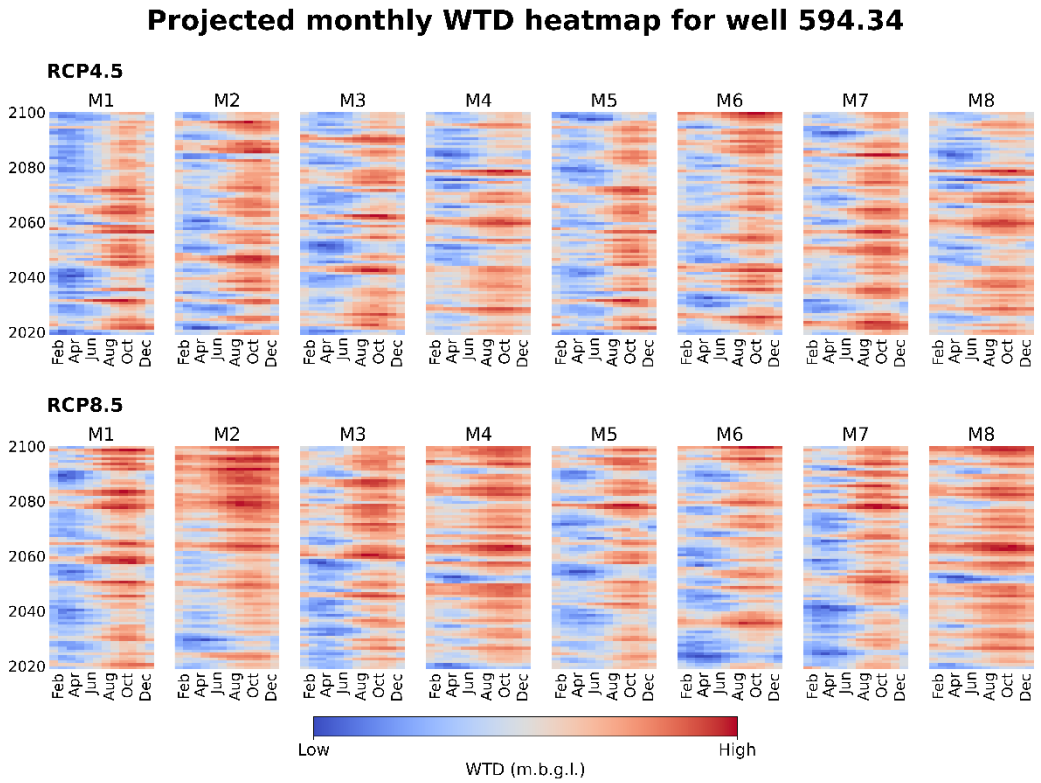

Figure 10. Heatmap plots for water table depth (WTD). RCP4.5 results in first and RCP8.5 in second row for one arbitrarily selected well (594.34) heatmap plots show the simulation period for each of the projections under each of the considered scenarios. Columns of each plot as months during the year and rows as the year (top: 2100-bottom: 2020).

produces more intense results than others, which is also true for the RCP4.5 scenario in the long run. It is also worth noting that all models exhibit the greatest degree of impact over the long-term period [2081-2100].

To provide a fresh perspective on the projection findings and the uncertainty resulting from future scenarios and models, we attempted to present the results as a median line, 25th-75th percentile area, and min-max area for both scenarios in the same plot. To smooth the findings, we computed all of these parameters based on the 5-year moving average of predictions (**Figure 11**).

Figure 11 shows that the decoupling of two scenarios occurs after the end of the reference period, but the major difference in water table depth occurs after the mid-term period, when the median line of RCP8.5 begins to deviate from the median line of RCP4.5, and this deviation increases as we approach the end of the century (long-term). Appendix 2 contains the findings of the heatmap of WTD and the median, 25th-75th range, and min-max range of 5-year moving average WTD for all 92 wells.

To compare the changes in WTD in each time period with respect to the reference period, we calculated the average of the medians under RCP8.5 related to each period (20 years) and showed the differences of each with respect to the reference period, and we plotted the results as a stacked bar chart for each well in meters on the map (**Figure 12**).

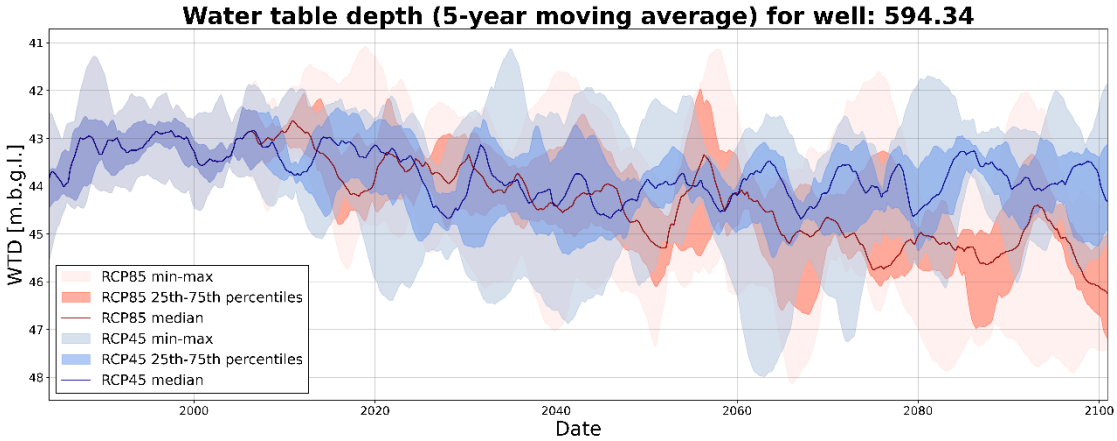

Figure 11. Water table depth 5-year moving average of 8 model medians, 25th-75th percentiles and min-max range for RCP4.5 and 8.5 for well (594.34).

Using the information in **Figure 12**, we can see that the changes linked to the long-term period are more substantial than the changes related to the near and mid-term periods. However, in the eastern area of Spain, long-term changes outnumber short-term and mid-term changes, and as we proceed to the central and western regions of the Iberian Peninsula, short-term and mid-term changes become more visible, particularly in the southern west region.

The obtained results on **Figure 13** inspired us to take a closer look at the changes in the long-term period under the RCP8.5 scenario, therefore we considered just the changes in the long-term period with regard to the reference

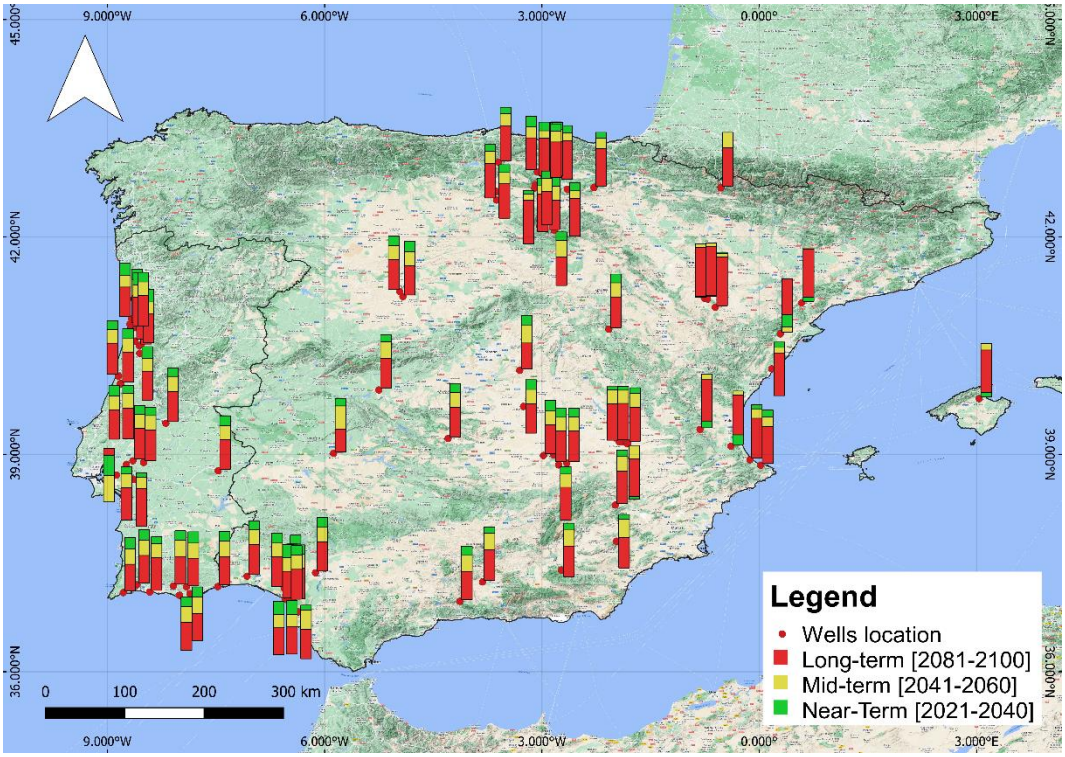

Figure 12. A stacked bar chart depicting the variations in WTD in meters across three distinct time periods under RCP8.5 in relation to the reference period.

period in meters and attempted to classify them based on magnitude. Looking at the data in **Figure 13**, we can see that even under RCP8.5, 5 (5.43%) of the wells have a recharge in WTD between 0 and 1 meter, while the remainder of the wells have a rise in WTD. The majority of wells have a depletion between 0 and 1 meter, which is 51 (55.43%). Highest depletion is 18.83 meters (well ID: 09.801.003), while maximum regeneration is 0.73 meters (well ID: 09.106.004).

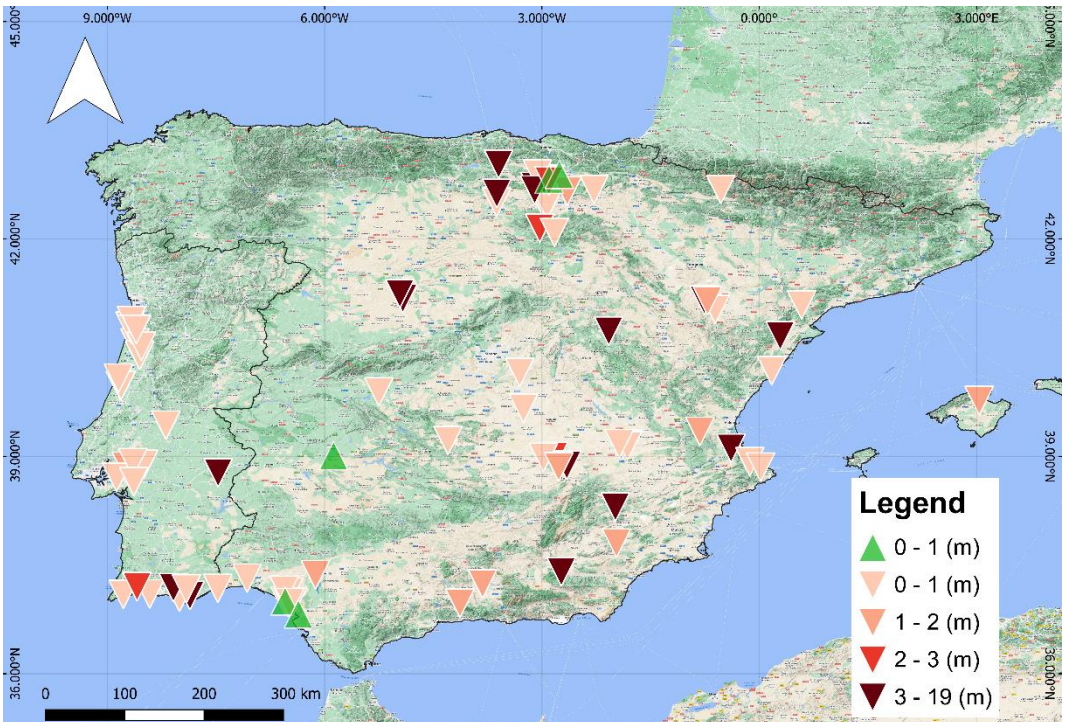

Figure 13. WTD changes in meters under RCP 8.5 in the long-term period [2081-2100] compared to the reference period [1986-2005].

Figure 14 shows the outcomes of the same plot for the RCP4.5 scenario over the long-term period. Within this figure 14, the regeneration of water table depth (indicated with green colors and upward triangles) is more common than in RCP8.5, and there are fewer instances of depletion as well.

By digging deeper into the results of **Figure 14**, regeneration wells are more frequent and with higher magnitudes, which are peaked in 1.51 m as the maximum regeneration and in quantity, there are 11 wells (11.96%) that are gaining water head and in contrast, looking at the depletion (red colored with downward triangles), they are still forming a greater quantity of wells but in terms of quality, they are less intense, where the maximum depletion here is 3.2 m and the majority of wells (67 well - 72.83%) had a depletion depth of 0 to 1 meter.

Furthermore, in order to better evaluate the distribution of these changes in WTD over time under two circumstances, we attempted to overlap the histogram

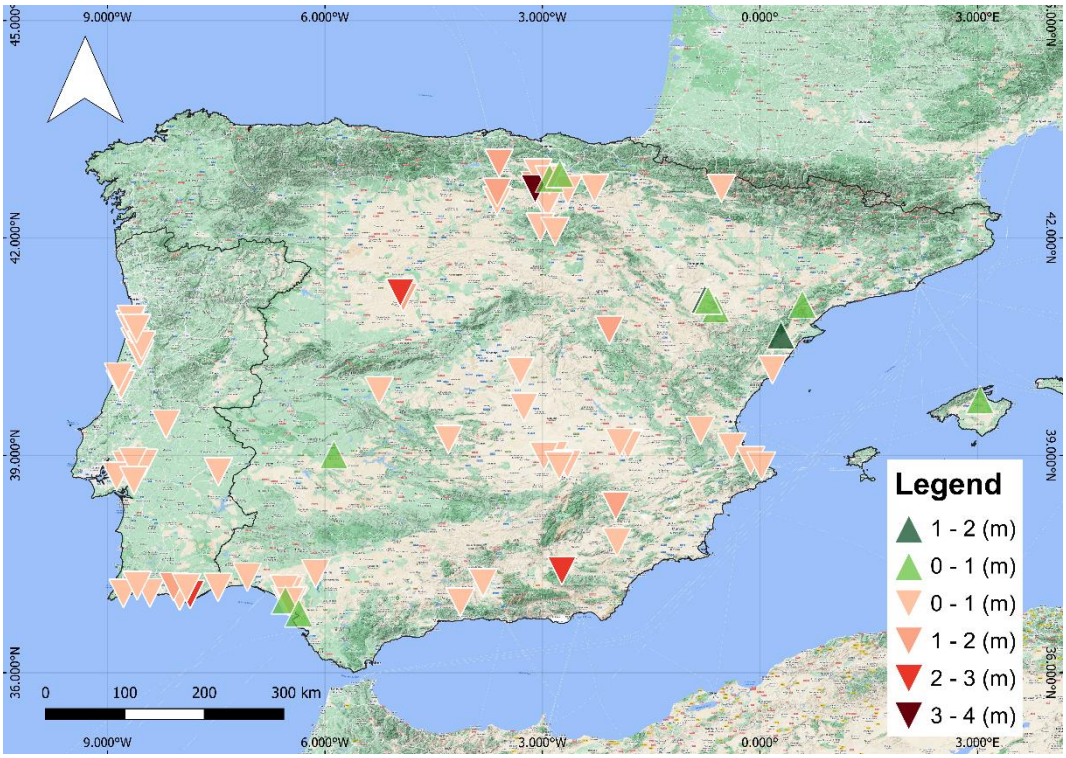

Figure 14. WTD changes in meters under RCP4.5 in the long-term period [2081-2100] compared to the reference period [1986-2005].

of these changes with the same bin size and numbers in order to have a better understanding of the results (**Figure 15**). The result clearly illustrates that the distribution of changes under RCP4.5 is compressed around zero, but the distribution of changes under RCP8.5 is right skewed (positively skewed) and has a significantly longer tail on the right side, indicating deeper alterations (**Figure 15**).

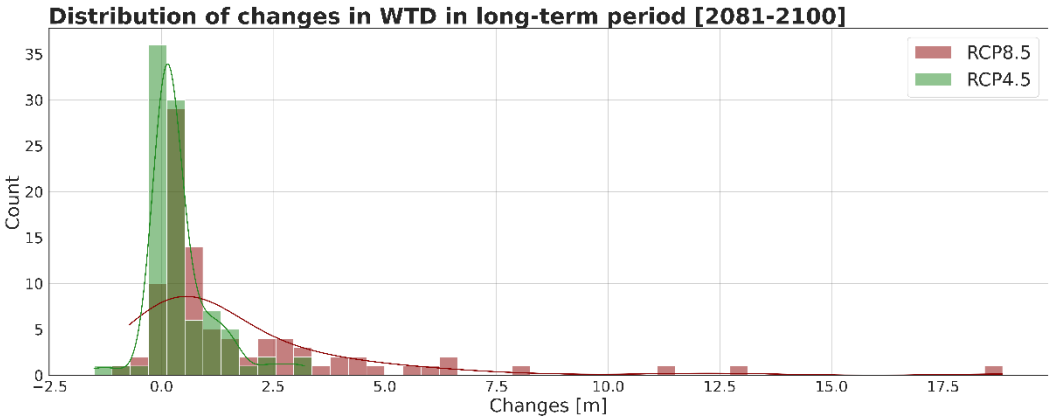

Figure 15. Histogram of changes in WTD in long-term period with respect to reference period under RCP4.5 and 8.5.

Chapter 5

Discussion and conclusions

In this study, we attempted to investigate the impact of climate change on GWLs of the Iberian Peninsula using a deep learning model. The objective was to assess the impact of different Representative Concentration Pathways (RCPs) on GWLs of the Iberian Peninsula and provide insights into future groundwater conditions. We used deep learning models to predict GWLs of 92 specific wells in the Iberian Peninsula. We trained the deep learning model using historical GWLs, climate data. We used two RCP scenarios (RCP4.5 and RCP8.5) to predict future GWLs under different greenhouse gas emission scenarios. RCP4.5 represents a future where greenhouse gas emissions are reduced, and RCP8.5 represents a future where greenhouse gas emissions continue to rise.

Our results showed that future GWLs are highly dependent on greenhouse gas emission scenarios. Under RCP8.5, we predicted more severe depletions of GWLs than under RCP4.5. In some cases, we predicted recharges as high as 1.5 meters under RCP4.5, whereas we estimated depletions under RCP8.5. These results clearly demonstrate that groundwater resource protection activities in RCP4.5 are effective and necessary. However, if the circumstances continue to be RCP8.5, we will most likely lose part of this valuable freshwater resource.

Our study highlights the importance of considering the impacts of climate change on GWLs in groundwater resource management. The use of AI and ML methods can provide valuable insights into future groundwater conditions, which can be used to develop effective groundwater management strategies. Our results also demonstrate the significant impact of greenhouse gas emission scenarios on GWLs. Therefore, it is crucial to reduce greenhouse gas emissions to mitigate the impacts of climate change on groundwater resources.

Capabilities of deep learning

Groundwater level (GWL) is a crucial parameter in hydrology, environmental management, and water resources planning. Traditionally, physically-based and numerical models have been used to simulate and predict GWL. However, these models require a deep understanding of the underlying topographic and hydro-geophysical factors, which can be time-consuming and expensive. Therefore, artificial intelligence (AI) models have emerged as a desirable methodology for predicting GWL. AI models are capable of simulating and predicting GWL without requiring a comprehensive understanding of the underlying factors. This makes AI models more accessible and easier to use than physically based and numerical models. Additionally, AI models have the potential to learn and adapt from data, making them more accurate over time [46]. Consequently, AI models have gained increasing attention from researchers and practitioners for predicting GWL, and their use is likely to increase in the future.

Several forms of AI, notably artificial neural network (ANN) and fuzzy logic, have been widely employed in engineering and science modelling in recent decades. Artificial intelligence's growth and uses in forecasting and monitoring groundwater quality and quantity are fast expanding [100]–[104]. AI has the benefit of lowering the time required for data sampling, and its ability to discover nonlinear patterns of input and output is more trustworthy than other traditional statistical approaches [105]. As a result, many academics have been drawn to the excellent precision and stability of AI structures in modelling complicated groundwater systems.

Deep learning, a subset of machine learning that specializes in producing outputs from unstructured input data using unsupervised learning methodologies, has grown in popularity in groundwater level simulation [106]. When compared to traditional data collecting, one of the key advantages of deep learning is the capacity to analyze complicated and high-dimensional data in a relatively short amount of time with minimum manpower [107].

Comparing to the German study

As compared to similar research done in Germany, our modelling findings demonstrate considerable declines in the GWLs of the analyzed wells. We discovered that in Germany, out of the 118 wells analyzed, 35 wells showed a drop in average change of the annual mean GWL of at least 9 cm, with 18 wells suffering

a decline ranging from -0.2 m to -2.1 m toward the end of the century under RCP8.5. This suggests that the groundwater resources in the Iberian Peninsula region are under severe stress as a result of the long-term effects of climate change compared to Germany.

Furthermore, we discovered that the majority of wells in Iberian Peninsula (51 out of 92 wells) had a depletion between 0 and 1 meter on average of the GWL median, emphasizing the severity of the situation in the region compared to Germany. Additionally, in the RCP8.5 scenario, the maximum depletion was 18.83 meters, according to our simulation results. These findings have significant implications for groundwater resource management in the research region, indicating the need for improved monitoring and conservation measures to maintain the sustainability of these resources in the face of future climate change impacts.

Other similar studies in the region

Groundwater is a vital freshwater resource that is relied upon by millions of people around the world. However, this resource is under threat from a variety of factors, including anthropogenic and climate change pressures. In recent years, various studies have been conducted to better understand the influence of climate change on groundwater levels, with most focusing on catchment-scale assessments using different approaches. The findings of these studies indicate that climate change does have an impact on groundwater levels. Still, this impact is not as significant as anthropic factors that contribute to resource depletion and scarcity. These anthropic factors can include excessive pumping, overuse, and poor management of groundwater resources.

According to [108], which has conducted research in the rural municipality of Abegondo in Galicia, the northern west part of Spain, where we don’t have any piezometer data available there, focusing on the sustainability of groundwater supplies in weathered and fractured schists. The study revealed that climate change might lower groundwater recharge by 6-10% by the end of the twenty-first century, aggravating water supply shortages during droughts, which is consistent with our overall, though not particular, findings. Overall, the study proposes groundwater management and protection actions such as land use planning and groundwater protection regulations based on a common consensus among all stakeholders involved, including local and regional authorities, agriculture planners, pig breeders, farmers, and water users.

Another research by [109] focuses on the Campina de Faro aquifer (M12) in southern Portugal (which we also have data available), where agricultural methods introduced in the 1970s resulted in high abstraction rates and salinization. Despite the fact that the EU Nitrates Regulation has been in effect since 1997, nitrate levels are still rising in some areas. The research creates a groundwater flow and mass transport model to examine nitrate evolution under various scenarios and anticipates the influence of climate change on groundwater levels. The results demonstrate a hydraulic relationship between M12 and the northernmost aquifers, and M12's reaction to excellent agricultural practices is gradual. Climate change might considerably influence groundwater levels, and massive drawdowns and hydraulic inversion would result in saltwater intrusion, rendering groundwater unsuitable for usage.

As a result, in our analysis, this location is one of the hotspots in terms of both time and intensity. In comparison to other places, this region will see the early signs of climate change on groundwater beginning in the near-term period (2021-2040), and the potential of saltwater intrusion is especially significant due to its proximity to the costal line.

The research [110] assesses the effects of climate change on the groundwater resources of Portugal's Serra da Estrela Mountain. The researchers predicted changes in hydrometeorological conditions from 1975 to 2005 using two climate scenarios, RCP4.5 and RCP8.5. They evaluated the effects of climate change by simulating daily temperature and precipitation values from climatic models and solving the daily hydrological water balance model with the VISUAL-BALAN tool. The findings indicate that the water resources in the Serra da Estrela Mountain basin will be extremely sensitive to expected changes in precipitation and temperature. Climate change will cause mean annual and monthly temperatures to rise considerably by the end of the twenty-first century, while precipitation will fall throughout the year, with the greatest relative decline occurring in the spring. Interflow, aquifer recharge, and streamflow will all decrease, with the greatest drop in mean monthly streamflows happening from March to May because of less rainfall and snowfall.

We do not have a specific model from the mountain region, but in the western part near the coastline, we have a significant number of well-trained models that all indicate a unified drop between 0 and 1 meter in the long-term period. The changes are visible beginning in the near and mid-term periods and peaking in the long-term.

The research [111] focuses on a Mediterranean region in Southeastern Spain, where groundwater resources are the principal supply of freshwater in dry and semi-arid areas. The researchers examined daily precipitation and monthly water level data series from several places around the region to determine the crucial threshold value for heavy precipitation events (HPEs) that result in significant aquifer recharging. The researchers used wavelet and trend analysis to investigate variations in the temporal distribution of HPEs and their anticipated development using 18 downscaled climate forecasts from 2040 to 2099. The precipitation time series were divided into ten groups based on commonalities determined by Pearson correlations. The findings revealed that the critical threshold for HPEs in the study area is 20 mm/day, and the number of HPEs producing appreciable aquifer recharge has decreased significantly in the last 60 years until 2012, a trend that is expected to be exacerbated by climate change by the end of the twenty-first century. The decline in HPEs is projected to lengthen no-aquifer-recharge times, highlighting groundwater shortage in the region. Province of Alicante decision-makers should use these findings when planning economic activities to manage groundwater resources in a sustainable manner.

We have several well-trained models in the Alicante province where the appearance of the impacts may not be adequately disclosed in the short and mid-term periods, but it is conceivable to witness some serious declines in GWLs in the long run. We noticed a decrease of 0 to 1 meter in two of the three wells in this location near the end of the century, but there is one well where the depth of the depletion exceeds 3 meters.

Limitations

While employing deep learning models such as 1D CNN networks to predict and forecast groundwater levels has certain advantages, there are some limits and possible issues to consider.

The quality and quantity of data provided are one of the most critical restrictions of utilizing any prediction model. In the case of groundwater level prediction, available data may be insufficient, or it may contain outliers, missing values, or mistakes that might impair forecast accuracy. We attempted to implement the outlier removal procedure using the generalized ESD test with a maximum of 10 outliers per time series data, but it was not possible to look at all of the outliers one by one, and because the groundwater data are not normally distributed, the results cannot be 100% correct.

While the model described here incorporates monthly temperature and precipitation data, as well as cumulative precipitation from different periods, it may not capture all of the key characteristics that determine groundwater levels. Additional factors such as soil type, terrain, vegetation cover, groundwater recharge rates, sea level pressure, relative humidity, wind speed, global radiation, and potential evaporation can all impact groundwater levels but may not be included in the model. This necessitates using a feature selection approach such as Correlation-based Feature Selection (CFS) [112], wrapper method [113], or embedded method [114]. The main problem with including several explanatory variables in the training of any machine learning model is the limited projection of all variables in future. So far, it is easier to project climate variables such as precipitation and temperature. However, other variables, such as relative humidity and land use adaptation, require further investigation to retrieve them under different future scenarios. This reflects the complementary of using process-based modelling together with the machine learning approach. When both approaches are used in parallel will open new horizons in investigating the direct and indirect impacts of climate change. Merging the flexibility of machine learning with the accuracy and physical process foundation of deterministic modelling will open new perspectives on groundwater assessment that were invisible when used separately.

Deep learning models are well-known for their capacity to discover complicated patterns and correlations in massive datasets. They can, however, be prone to overfitting, particularly when the number of training samples is limited in comparison to the number of input characteristics. This might result in a model that does well on training data but does not generalize well to fresh data. Despite the fact that we utilized a Monte-Carlo dropout layer for each of the ten ensemble members, with a fixed dropout of 50% to keep the model from overfitting.

Conclusion

In the RCP8.5 scenario, our models reveal a relatively significant regional reduction in climate-driven groundwater levels by the end of the century. The results for RCP4.5, however, showed less substantial changes. Even though a drop of a small level (depending on the projection and area) might be critical for sustainable groundwater management, especially for groundwater-dependent ecosystems during low-flow conditions when groundwater is no longer available.

Our results show that the eastern part of the Iberian Peninsula has more dominance on GWL depletion in the long-term period compared to the near and

mid-term periods, and as we move to central and the south-western part of the region, we see that the depletion is becoming more visible in the near and mid-term periods, implying that the impact of climate change on groundwater level is site-specific and will be revealed earlier in the western and southern west parts of the Iberian Peninsula under RCP8.5. Our findings reveal that under the RCP8.5 scenario, which is the worst-case scenario, groundwater levels would drop by around one meter for 55 wells out of total 92 by the end of the century, highlighting the resource's resilience to climate change for future human usage. As a result, it is necessary to put in place management strategies to limit the pumping rate and assure the long-term usage of this vital resource.

Groundwater levels can be affected by climate change in both direct and indirect ways. With its indeterministic foundation, our model omits any process-based conceptualization of groundwater behaviour and will focus only on the direct impact of climate change effects. Our modelling results clearly showed that the projected changes in groundwater levels in the Iberian Peninsula due to only the direct effects of climate change (through temperature and precipitation) are much smaller than any anthropogenic changes (overexploitation) experienced in the Iberian Peninsula currently and in the last decades. For instance, the average depletion of all groundwater wells by 2100 under the RCP8.5 is about 1 m, which is presently experienced only in one year period in many groundwater systems in the Iberian Peninsula due to the unstainable human use.

The indirect impact of climate change through the overpumping for irrigation to mitigate the induced drought conditions is more severe than any direct impact of climate change on groundwater systems through precipitation and temperature. Nevertheless, the indirect impact, such as increased pumping owing to a shortage of surface water for irrigation, may have a greater influence in future as the region's food need grows. The region is currently experiencing severe groundwater depletion in many aquifers, reflecting the urgent need for more sustainable use of groundwater resources.

Appendix 1

Provided in the portal as a separate file, including hyperparameters, extremes and SHAP summary plots for the 92 studied wells.

Appendix 2

Provided in the portal as a separate file, including water table depth (WTD) 5-year moving average of eight model medians, 25th-75th percentiles and min-max range and heatmap plots for RCP4.5 and 8.5 scenarios for the 92 studied wells.

Acknowledgement

This work was supported by InTheMED PRIMA Program project funded by the European Union's Horizon 2020 research and innovation under grant agreement No 1923.

References

[1] R. G. Taylor *et al.*, "Ground water and climate change," *Nature Climate Change 2012 3:4*, vol. 3, no. 4, pp. 322–329, Nov. 2012, doi: 10.1038/nclimate1744.

[2] C. Leduc, A. Pulido-Bosch, and B. Remini, "Anthropization of groundwater resources in the Mediterranean region: processes and challenges," *Hydrogeology Journal 2017 25:6*, vol. 25, no. 6, pp. 1529–1547, Apr. 2017, doi: 10.1007/S10040-017-1572-6.

[3] J. M. García-Ruiz, I. I. López-Moreno, S. M. Vicente-Serrano, T. Lasanta-Martínez, and S. Beguería, "Mediterranean water resources in a global change scenario," *Earth Sci Rev*, vol. 105, no. 3–4, pp. 121–139, Apr. 2011, doi: 10.1016/J.EARSCIREV.2011.01.006.

[4] G. Basin *et al.*, "Evaluation of Bayesian Networks in Participatory Water Resources Management, Upper Guadiana Basin, Spain," and Society, 2010. [Online]. Available: https://www.jstor.org/stable/26268156

[5] M. Jesús Aira *et al.*, "Cladosporium airborne spore incidence in the environmental quality of the Iberian Peninsula," *http://dx.doi.org/10.1080/00173134.2012.717636*, vol. 51, no. 4, pp. 293–304, Dec. 2012, doi: 10.1080/00173134.2012.717636.

[6] P. Zhang, B. Anderson, M. Barlow, B. Tan, and R. B. Myneni, "Climate-related vegetation characteristics derived from Moderate Resolution Imaging Spectroradiometer (MODIS) leaf area index and normalized difference vegetation index," *Journal of Geophysical Research D: Atmospheres*, vol. 109, no. 20, Oct. 2004, doi: 10.1029/2004JD004720.

[7] T. J. Kwiatkowski *et al.*, "Mutations in the FUS/TLS gene on chromosome 16 cause familial amyotrophic lateral sclerosis," *Science (1979)*, vol. 323, no. 5918, pp. 1205–1208, Feb. 2009, doi: 10.1126/SCIENCE.1166066/SUPPL_FILE/KWIATKOWSKI-SOM.PDF.

[8] D. Viviroli and R. Weingartner, “The hydrological significance of mountains: from regional to global scale,” *Hydrol Earth Syst Sci*, vol. 8, no. 6, pp. 1017–1030, Dec. 2004, doi: 10.5194/HESS-8-1017-2004.

[9] B. Messerli and J. D. Ives, “Mountains of the world: a global priority,” 1997, doi: 10.3/JQUERY-UI.JS.

[10] D. Viviroli, H. H. Dürr, B. Messerli, M. Meybeck, and R. Weingartner, “Mountains of the world, water towers for humanity: Typology, mapping, and global significance,” *Water Resour Res*, vol. 43, no. 7, p. 7447, Jul. 2007, doi: 10.1029/2006WR005653.

[11] F. Gallart and P. Llorens, “Water resources and environmental change in Spain. A key issue for sustainable integrated catchment management,” *Cuadernos de Investigación Geográfica*, vol. 27, pp. 7–16, May 2001, doi: 10.18172/CIG.1109.

[12] “The National Statistics Institute of Spain,” 2008. https://www.ine.es/en/ (accessed Jan. 10, 2023).

[13] F. López-Vera, “Groundwater: The Invisible Resource,” *Int J Water Resour Dev*, vol. 28, no. 1, pp. 141–150, Mar. 2012, doi: 10.1080/07900627.2012.642238.

[14] M. Sala, “HYDROGEOMORPHOLOGICAL ASSESSMENT OF SURFACE AND GROUNDWATER QUALITY IN THE RIDAURA STREAM, CATALAN RANGES, NE IBERIAN PENINSULA,” *& development Land Degrad. Develop*, vol. 15, pp. 311–323, 2004, doi: 10.1002/ldr.615.

[15] N. Alfarrah and K. Walraevens, “Groundwater overexploitation and seawater intrusion in coastal areas of arid and semi-arid regions,” *Water (Switzerland)*, vol. 10, no. 2, Feb. 2018, doi: 10.3390/W10020143.

[16] R. K. Pachauri *et al.*, “Climate Change 2014: Synthesis Report. Contribution of Working Groups I, II and III to the Fifth Assessment Report of the Intergovernmental Panel on Climate Change,” *EPIC3Geneva, Switzerland, IPCC, 151 p., pp. 151, ISBN: 978-92-9169-143-2*, 2014, Accessed: Jan. 09, 2023. [Online]. Available: https://www.ipcc.ch/pdf/assessment-report/ar5/syr/SYR_AR5_FINAL_full_wcover.pdf

[17] S. Michaelides *et al.*, “Reviews and perspectives of high impact atmospheric processes in the Mediterranean,” *Atmos Res*, vol. 208, pp. 4–44, Aug. 2018, doi: 10.1016/J.ATMOSRES.2017.11.022.

[18] “Analytic Element Modeling of Groundwater Flow - H. M. Haitjema - Google Books.” https://books.google.it/books?hl=en&lr=&id=lzoPUX_zD6gC&oi=fnd&pg=PP1&dq=+Haitjema,+H.+M.+(Henk+M.)+(1995).+Analytic+element+modeling+of+groundwater+flow.+San+Diego:+Academic+Press.&ots=DKR5ilxH1C&sig=I_qn0pHhzVkObZQfkx-NDV8uuHM&redir_esc=y#v=onepage&q=Haitjema%2C%20H.%20M.%20(Henk%20M.)%20(1995).%20Analytic%20element%20modeling%20of%20groundwater%20flow.%20San%20Diego%3A%20Academic%20Press.&f=false (accessed Jan. 09, 2023).

[19] “Analytical Groundwater Mechanics - Otto D. L. Strack - Google Books.” https://books.google.it/books?hl=en&lr=&id=j_8wDwAAQBAJ&oi=fnd&pg=PR9&dq=Strack,+Otto+D.+L.+(August+2017).+Analytical+Groundwater+Mechanics.+Cambridge+Core.&ots=yeN8f1U_NS&sig=nqKpt_t70zIOumSb6A7XPBVTtZM&redir_esc=y#v=onepage&q&f=false (accessed Jan. 09, 2023).

[20] O. D. L. Strack, “Groundwater mechanics,” p. 732, 1989, doi: 10.3/JQUERY-UI.JS.

[21] J. Dupuit, *Etudes théoriques et pratiques sur le mouvement des eaux dans les canaux découverts et à travers les terrains perméables avec des considérations relatives*. 1863. Accessed: Mar. 03, 2023. [Online]. Available: https://books.google.com/books?hl=en&lr=&id=aTR4r0JbfyQC&oi=fnd&pg=PA28&dq=Etudes+Theoriques+et+Pratiques+sur+le+Mouvement+des+Eaux+dans+les+Canaux+Decouverts+et+a+Travers+les+Terrains+Permeables&ots=xzYXVaPuY0&sig=C9easYmbBCQTKn1CffVn0E_AGYQ

[22] M. S. Hantush and C. E. Jacob, “Non-steady radial flow in an infinite leaky aquifer,” *Eos, Transactions American Geophysical Union*, vol. 36, no. 1, pp. 95–100, Feb. 1955, doi: 10.1029/TR036I001P00095.

[23] “Dynamics of Fluids in Porous Media - Jacob Bear - Google Books.” https://books.google.it/books?hl=en&lr=&id=fBMeVSZ_3u8C&oi=fnd&p

g=PP1&dq=Dynamics+of+Fluids+in+Porous+Media%22+(1972,&ots=mhhCBjUHLC&sig=Ml19G-gK2Au6ENBzgZJx3N1Ca4g&redir_esc=y#v=onepage&q=Dynamics%20of%20Fluids%20in%20Porous%20Media%22%20(1972%2C&f=false (accessed Mar. 03, 2023).

[24] M. G. McDonald and A. W. Harbaugh, "The History of MODFLOW," *Groundwater*, vol. 41, no. 2, pp. 280–283, Mar. 2003, doi: 10.1111/J.1745-6584.2003.TB02591.X.

[25] H. J. G. Diersch, "FEFLOW: Finite element modeling of flow, mass and heat transport in porous and fractured media," *FEFLOW: Finite Element Modeling of Flow, Mass and Heat Transport in Porous and Fractured Media*, vol. 9783642387395, pp. 1–996, Aug. 2014, doi: 10.1007/978-3-642-38739-5.

[26] S. W. Mehl and M. C. Hill, "MODFLOW-2005, the U.S. Geological Survey modular ground-water model - documentation of shared node local grid refinement (LGR) and the boundary flow and head (BFH) package," *Techniques and Methods*, 2006, doi: 10.3133/TM6A12.

[27] C. 1962- Zheng and P. Patrick. Wang, "MT3DMS : a modular three-dimensional multispecies transport model for simulation of advection, dispersion, and chemical reactions of contaminants in groundwater systems; documentation and user's guide," *This Digital Resource was created in Microsoft Word and Adobe Acrobat*, 1999, Accessed: Mar. 03, 2023. [Online]. Available: https://erdc-library.erdc.dren.mil/jspui/handle/11681/4734

[28] N. K. C. Twarakavi, J. Šimůnek, and S. Seo, "Evaluating Interactions between Groundwater and Vadose Zone Using the HYDRUS-Based Flow Package for MODFLOWAll rights reserved. No part of this periodical may be reproduced or transmitted in any form or by any means, electronic or mechanical, including photocopying, recording, or any information storage and retrieval system, without permission in writing from the publisher.," *Vadose Zone Journal*, vol. 7, no. 2, pp. 757–768, May 2008, doi: 10.2136/VZJ2007.0082.

[29] A. Wunsch, T. Liesch, and S. Broda, "Deep learning shows declining groundwater levels in Germany until 2100 due to climate change," *Nature*

Communications 2022 13:1, vol. 13, no. 1, pp. 1–13, Mar. 2022, doi: 10.1038/s41467-022-28770-2.

[30] Y. Wada, L. P. H. van Beek, C. M. van Kempen, J. W. T. M. Reckman, S. Vasak, and M. F. P. Bierkens, "Global depletion of groundwater resources," *Geophys Res Lett*, vol. 37, no. 20, Oct. 2010, doi: 10.1029/2010GL044571.

[31] M. Qadir, B. R. Sharma, A. Bruggeman, R. Choukr-Allah, and F. Karajeh, "Non-conventional water resources and opportunities for water augmentation to achieve food security in water scarce countries," *Agric Water Manag*, vol. 87, no. 1, pp. 2–22, Jan. 2007, doi: 10.1016/J.AGWAT.2006.03.018.

[32] S. Sadeghi-Tabas, S. Z. Samadi, and B. Zahabiyoun, "Application of Bayesian algorithm in continuous streamflow modeling of a mountain watershed," *European Water*, vol. 57, pp. 101–108, 2017.

[33] H. Afzaal, A. A. Farooque, F. Abbas, B. Acharya, and T. Esau, "Groundwater Estimation from Major Physical Hydrology Components Using Artificial Neural Networks and Deep Learning," *Water 2020, Vol. 12, Page 5*, vol. 12, no. 1, p. 5, Dec. 2019, doi: 10.3390/W12010005.

[34] J. Wiley, N. York, K. Terzaghi, and R. B. Peck, "SOIL MECHANICS IN ENGINEERING PRACTICE".

[35] "Etudes théoriques et pratiques sur le mouvement des eaux dans les canaux ... - Jules Etienne Dupuit - Google Books." https://books.google.it/books?hl=en&lr=&id=aTR4r0JbfyQC&oi=fnd&pg=PA28&dq=Dupuit,+J.+(1863).+Etudes+Th%C3%A9oriques+et+Pratiques+sur+le+mouvement+des+Eaux+dans+les+canaux+d%C3%A9couverts+et+%C3%A0+travers+les+terrains+perm%C3%A9ables+(Second+ed.).+Paris:+Dunod.&ots=xzYTRaPzY3&sig=mir3ndZbG3l9KWiYQtGbsUE74iw&redir_esc=y#v=onepage&q=Dupuit%2C%20J.%20(1863).%20Etudes%20Th%C3%A9oriques%20et%20Pratiques%20sur%20le%20mouvement%20des%20Eaux%20dans%20les%20canaux%20d%C3%A9couverts%20et%20%C3%A0%20travers%20les%20terrains%20perm%C3%A9ables%20(Second%20ed.).%20Paris%3A%20Dunod.&f=false (accessed Jan. 11, 2023).

[36] C. v. Theis, "The relation between the lowering of the Piezometric surface and the rate and duration of discharge of a well using ground-water storage,"

Eos, Transactions American Geophysical Union, vol. 16, no. 2, pp. 519–524, Aug. 1935, doi: 10.1029/TR016I002P00519.

[37] M. S. Hantush and C. E. Jacob, "Non-steady green's functions for an infinite strip of leaky aquifer," *Eos, Transactions American Geophysical Union*, vol. 36, no. 1, pp. 101–112, Feb. 1955, doi: 10.1029/TR036I001P00101.

[38] D. W. Pollock, "User guide for MODPATH Version 7—A particle-tracking model for MODFLOW," *Open-File Report*, 2016, doi: 10.3133/OFR20161086.

[39] R. G. Niswonger, S. Panday, and M. Ibaraki, "MODFLOW-NWT, A Newton formulation for MODFLOW-2005," *Techniques and Methods*, 2011, doi: 10.3133/TM6A37.

[40] V. Bedekar, E. D. Morway, C. D. Langevin, and M. J. Tonkin, "MT3D-USGS version 1: A U.S. Geological Survey release of MT3DMS updated with new and expanded transport capabilities for use with MODFLOW," *Techniques and Methods*, 2016, doi: 10.3133/TM6A53.

[41] B. Barnett, L. R. Townley, and L. Peeters, "Developing Groundwater Modelling Guidelines for Australia," 2013, Accessed: Feb. 13, 2023. [Online]. Available: https://i2insights.org/2016/12/01/strength-of-failing/

[42] H. Tao *et al.*, "Groundwater level prediction using machine learning models: A comprehensive review," *Neurocomputing*, vol. 489, pp. 271–308, Jun. 2022, doi: 10.1016/J.NEUCOM.2022.03.014.

[43] J. Adamowski and H. F. Chan, "A wavelet neural network conjunction model for groundwater level forecasting," *J Hydrol (Amst)*, vol. 407, no. 1–4, pp. 28–40, Sep. 2011, doi: 10.1016/j.jhydrol.2011.06.013.

[44] B. Barnett, L. R. Townley, and L. Peeters, "Developing Groundwater Modelling Guidelines for Australia Integrated Water Management View project Modelling of groundwater flow and solute transport in regional scale aquifers View project," 2013, Accessed: Feb. 17, 2023. [Online]. Available: https://www.researchgate.net/publication/277711322

[45] H. Park, K. Kim, and D. K. Lee, "Prediction of Severe Drought Area Based on Random Forest: Using Satellite Image and Topography Data," *Water*

2019, Vol. 11, Page 705, vol. 11, no. 4, p. 705, Apr. 2019, doi: 10.3390/W11040705.

[46] J. Adamowski and H. F. Chan, "A wavelet neural network conjunction model for groundwater level forecasting," *J Hydrol (Amst)*, vol. 407, no. 1–4, pp. 28–40, Sep. 2011, doi: 10.1016/J.JHYDROL.2011.06.013.

[47] S. Afrifa, T. Zhang, P. Appiahene, and V. Varadarajan, "Mathematical and Machine Learning Models for Groundwater Level Changes: A Systematic Review and Bibliographic Analysis," *Future Internet 2022, Vol. 14, Page 259*, vol. 14, no. 9, p. 259, Aug. 2022, doi: 10.3390/FI14090259.

[48] X. Yang, H. Zhang, and H. Zhou, "A Hybrid Methodology for Salinity Time Series Forecasting Based on Wavelet Transform and NARX Neural Networks," *Arab J Sci Eng*, vol. 39, no. 10, pp. 6895–6905, Sep. 2014, doi: 10.1007/S13369-014-1243-Z/METRICS.

[49] S. Sahoo, T. A. Russo, J. Elliott, and I. Foster, "Machine learning algorithms for modeling groundwater level changes in agricultural regions of the U.S.," *Water Resour Res*, vol. 53, no. 5, pp. 3878–3895, May 2017, doi: 10.1002/2016WR019933.

[50] J. Chang, G. Wang, and T. Mao, "Simulation and prediction of suprapermafrost groundwater level variation in response to climate change using a neural network model," *J Hydrol (Amst)*, vol. 529, pp. 1211–1220, Oct. 2015, doi: 10.1016/J.JHYDROL.2015.09.038.

[51] Z. Gaffoor, A. Gritzman, K. Pietersen, N. Jovanovic, A. Bagula, and T. Kanyerere, "An autoregressive machine learning approach to forecast high-resolution groundwater-level anomalies in the Ramotswa/North West/Gauteng dolomite aquifers of Southern Africa," *Hydrogeol J*, vol. 30, no. 2, pp. 575–600, Mar. 2022, doi: 10.1007/S10040-021-02439-4/FIGURES/14.

[52] P. J. Jyolsna, B. V. N. P. Kambhammettu, and S. Gorugantula, "Application of random forest and multi-linear regression methods in downscaling GRACE derived groundwater storage changes," *https://doi.org/10.1080/02626667.2021.1896719*, vol. 66, no. 5, pp. 874–887, 2021, doi: 10.1080/02626667.2021.1896719.

[53] T. Paepae, P. N. Bokoro, and K. Kyamakya, “From Fully Physical to Virtual Sensing for Water Quality Assessment: A Comprehensive Review of the Relevant State-of-the-Art,” *Sensors 2021, Vol. 21, Page 6971*, vol. 21, no. 21, p. 6971, Oct. 2021, doi: 10.3390/S21216971.

[54] L. Shi, H. Gong, B. Chen, and C. Zhou, “Land Subsidence Prediction Induced by Multiple Factors Using Machine Learning Method,” *Remote Sensing 2020, Vol. 12, Page 4044*, vol. 12, no. 24, p. 4044, Dec. 2020, doi: 10.3390/RS12244044.

[55] S. S. Band *et al.*, “Comparative Analysis of Artificial Intelligence Models for Accurate Estimation of Groundwater Nitrate Concentration,” *Sensors 2020, Vol. 20, Page 5763*, vol. 20, no. 20, p. 5763, Oct. 2020, doi: 10.3390/S20205763.

[56] S. Lee, K. K. Lee, and H. Yoon, “Using artificial neural network models for groundwater level forecasting and assessment of the relative impacts of influencing factors,” *Hydrogeol J*, vol. 27, no. 2, pp. 567–579, Mar. 2019, doi: 10.1007/S10040-018-1866-3/FIGURES/9.

[57] B. Yadav, P. K. Gupta, N. Patidar, and S. K. Himanshu, “Ensemble modelling framework for groundwater level prediction in urban areas of India,” *Science of The Total Environment*, vol. 712, p. 135539, Apr. 2020, doi: 10.1016/J.SCITOTENV.2019.135539.

[58] M. Sit, B. Z. Demiray, Z. Xiang, G. J. Ewing, Y. Sermet, and I. Demir, “A comprehensive review of deep learning applications in hydrology and water resources,” *Water Science and Technology*, vol. 82, no. 12, pp. 2635–2670, Dec. 2020, doi: 10.2166/WST.2020.369.

[59] D. Kumar, T. Roshni, A. Singh, M. K. Jha, and P. Samui, “Predicting groundwater depth fluctuations using deep learning, extreme learning machine and Gaussian process: a comparative study,” *Earth Sci Inform*, vol. 13, no. 4, pp. 1237–1250, Dec. 2020, doi: 10.1007/S12145-020-00508-Y/TABLES/4.

[60] B. S. Supreetha, N. Shenoy, and P. Nayak, “Lion Algorithm-Optimized Long Short-Term Memory Network for Groundwater Level Forecasting in Udupi District, India,” *Applied Computational Intelligence and Soft Computing*, vol. 2020, 2020, doi: 10.1155/2020/8685724.

[61] M. T. Vu, A. Jardani, N. Massei, and M. Fournier, “Reconstruction of missing groundwater level data by using Long Short-Term Memory (LSTM) deep neural network,” *J Hydrol (Amst)*, vol. 597, p. 125776, Jun. 2021, doi: 10.1016/J.JHYDROL.2020.125776.

[62] A. Y. Sun *et al.*, “Combining Physically Based Modeling and Deep Learning for Fusing GRACE Satellite Data: Can We Learn From Mismatch?,” *Water Resour Res*, vol. 55, no. 2, pp. 1179–1195, Feb. 2019, doi: 10.1029/2018WR023333.

[63] J. Jeong, E. Park, H. Chen, K. Y. Kim, W. Shik Han, and H. Suk, “Estimation of groundwater level based on the robust training of recurrent neural networks using corrupted data,” *J Hydrol (Amst)*, vol. 582, p. 124512, Mar. 2020, doi: 10.1016/J.JHYDROL.2019.124512.

[64] A. Zhang, J. Winterle, and C. Yang, “Performance comparison of physical process-based and data-driven models: a case study on the Edwards Aquifer, USA,” *Hydrogeol J*, vol. 28, no. 6, pp. 2025–2037, Sep. 2020, doi: 10.1007/S10040-020-02169-Z/FIGURES/7.

[65] J. Müller *et al.*, “Surrogate optimization of deep neural networks for groundwater predictions,” *Journal of Global Optimization*, vol. 81, no. 1, pp. 203–231, Sep. 2021, doi: 10.1007/S10898-020-00912-0/FIGURES/10.

[66] J. Jeong and E. Park, “Comparative applications of data-driven models representing water table fluctuations,” *J Hydrol (Amst)*, vol. 572, pp. 261–273, May 2019, doi: 10.1016/J.JHYDROL.2019.02.051.

[67] S. M. Guzman, J. O. Paz, and M. L. M. Tagert, “The Use of NARX Neural Networks to Forecast Daily Groundwater Levels,” *Water Resources Management*, vol. 31, no. 5, pp. 1591–1603, Mar. 2017, doi: 10.1007/S11269-017-1598-5/TABLES/2.

[68] A. Wunsch, T. Liesch, and S. Broda, “Groundwater level forecasting with artificial neural networks: A comparison of long short-term memory (LSTM), convolutional neural networks (CNNs), and non-linear autoregressive networks with exogenous input (NARX),” *Hydrol Earth Syst Sci*, vol. 25, no. 3, pp. 1671–1687, Apr. 2021, doi: 10.5194/HESS-25-1671-2021.

[69] S. M. Guzman, J. O. Paz, M. Love, and M. Tagert, “The Use of NARX Neural Networks to Forecast Daily Groundwater Levels,” vol. 31, pp. 1591–1603, 2017, doi: 10.1007/s11269-017-1598-5.

[70] J. Jeong and E. Park, “Comparative applications of data-driven models representing water table fluctuations,” *J Hydrol (Amst)*, vol. 572, pp. 261–273, May 2019, doi: 10.1016/j.jhydrol.2019.02.051.

[71] J. Müller *et al.*, “Surrogate optimization of deep neural networks for groundwater predictions,” *Journal of Global Optimization*, vol. 81, pp. 203–231, 2021, doi: 10.1007/s10898-020-00912-0.

[72] A. Zhang, J. Winterle, and C. Yang, “Performance comparison of physical process-based and data-driven models: a case study on the Edwards Aquifer, USA,” *Hydrogeol J*, vol. 28, no. 6, pp. 2025–2037, Sep. 2020, doi: 10.1007/s10040-020-02169-z.

[73] J. Jeong, E. Park, H. Chen, K. Y. Kim, W. Shik Han, and H. Suk, “Estimation of groundwater level based on the robust training of recurrent neural networks using corrupted data,” *J Hydrol (Amst)*, vol. 582, Mar. 2020, doi: 10.1016/j.jhydrol.2019.124512.

[74] F. Kratzert, M. Herrnegger, D. Klotz, S. Hochreiter, and G. Klambauer, “NeuralHydrology – Interpreting LSTMs in Hydrology,” *Lecture Notes in Computer Science (including subseries Lecture Notes in Artificial Intelligence and Lecture Notes in Bioinformatics)*, vol. 11700 LNCS, pp. 347–362, 2019, doi: 10.1007/978-3-030-28954-6_19.

[75] F Nogueira, “Bayesian Optimization: Open source constrained global optimization tool for Python,” 2014. https://github.com/fmfn/BayesianOptimization (accessed Jan. 12, 2023).

[76] “Python Tutorial Release 3.8.1 Guido van Rossum and the Python development team,” 2020.

[77] M. Abadi *et al.*, “TensorFlow: Large-Scale Machine Learning on Heterogeneous Distributed Systems,” Mar. 2016, doi: 10.48550/arxiv.1603.04467.

[78] F. Chollet, “keras,” 2015. https://github.com/fchollet/keras (accessed Jan. 12, 2023).

[79] S. van der Walt, S. C. Colbert, and G. Varoquaux, “The NumPy array: A structure for efficient numerical computation,” *Comput Sci Eng*, vol. 13, no. 2, pp. 22–30, Mar. 2011, doi: 10.1109/MCSE.2011.37.

[80] W. Mckinney, “Data Structures for Statistical Computing in Python,” 2010.

[81] T. pandas development team, “pandas-dev/pandas: Pandas,” Nov. 2022, doi: 10.5281/ZENODO.7344967.

[82] F. Pedregosa FABIANPEDREGOSA *et al.*, “Scikit-learn: Machine Learning in Python Gaël Varoquaux Bertrand Thirion Vincent Dubourg Alexandre Passos PEDREGOSA, VAROQUAUX, GRAMFORT ET AL. Matthieu Perrot,” *Journal of Machine Learning Research*, vol. 12, pp. 2825–2830, 2011, Accessed: Jan. 12, 2023. [Online]. Available: http://scikit-learn.sourceforge.net.

[83] “fmfn/BayesianOptimization: A Python implementation of global optimization with gaussian processes.” https://github.com/fmfn/BayesianOptimization (accessed Jan. 12, 2023).

[84] J. D. Hunter, “Matplotlib: A 2D Graphics Environment,” *Comput Sci Eng*, vol. 9, no. 03, pp. 90–95, May 2007, doi: 10.1109/MCSE.2007.55.

[85] “Welcome to the uncertainties package — uncertainties Python package 3.0.1 documentation.” https://pythonhosted.org/uncertainties/ (accessed Jan. 12, 2023).

[86] “Outlier detection — PyAstronomy 0.19.0beta documentation.” https://pyastronomy.readthedocs.io/en/latest/pyaslDoc/aslDoc/outlier.html#PyAstronomy.pyasl.generalizedESD (accessed Jan. 18, 2023).

[87] S. M. Lundberg and S.-I. Lee, “A Unified Approach to Interpreting Model Predictions,” 2017.

[88] S. Herrera, R. Margarida Cardoso, P. Matos Soares, F. Espírito-Santo, P. Viterbo, and J. M. Gutiérrez, “Iberia01: A new gridded dataset of daily precipitation and temperatures over Iberia,” *Earth Syst Sci Data*, vol. 11, no. 4, pp. 1947–1956, Dec. 2019, doi: 10.5194/ESSD-11-1947-2019.

[89] S. Herrera, J. Fernández, and J. M. Gutiérrez, “Update of the Spain02 gridded observational dataset for EURO-CORDEX evaluation: Assessing the effect

of the interpolation methodology," *International Journal of Climatology*, vol. 36, no. 2, pp. 900–908, Feb. 2016, doi: 10.1002/JOC.4391.

[90] "Red de seguimiento piezométrico." https://www.miteco.gob.es/es/agua/temas/evaluacion-de-los-recursos-hidricos/red-oficial-seguimiento/Red-seguimiento-piezometrico.aspx (accessed Jan. 13, 2023).

[91] "Redes de Seguimiento del Estado e Información Hidrológica." https://sig.mapama.gob.es/redes-seguimiento/index.html?herramienta=Piezometros (accessed Jan. 13, 2023).

[92] "SNIRH > Dados de Base." https://snirh.apambiente.pt/index.php?idMain=2&idItem=1 (accessed Jan. 13, 2023).

[93] "SNIRH :: Sistema Nacional de Informação de Recursos Hídricos." https://snirh.apambiente.pt/ (accessed Jan. 13, 2023).

[94] M. Kuppusamy, S. Kannan Kaliyaperumal, and S. K. Kannan, "Comparison of Methods for detecting Outliers Comparative analysis of community discovery methods in social networks View project Comparison of methods for detecting outliers," 2013, [Online]. Available: http://www.ijser.org

[95] F. J. Anscombe and I. Guttman, "Rejection of Outliers," *Technometrics*, vol. 2, no. 2, p. 123, May 1960, doi: 10.2307/1266540.

[96] B. Rosner, "Percentage points for a generalized esd many-outlier procedure," *Technometrics*, vol. 25, no. 2, pp. 165–172, 1983, doi: 10.1080/00401706.1983.10487848.

[97] "1.3.5.17.3. Generalized Extreme Studentized Deviate Test for Outliers." https://www.itl.nist.gov/div898/handbook/eda/section3/eda35h3.htm (accessed Jan. 18, 2023).

[98] S. Duan, P. Ullrich, and L. Shu, "Using Convolutional Neural Networks for Streamflow Projection in California," *Frontiers in Water*, vol. 2, p. 28, Sep. 2020, doi: 10.3389/FRWA.2020.00028/BIBTEX.

[99] J. Wu, X. Y. Chen, H. Zhang, L. D. Xiong, H. Lei, and S. H. Deng, "Hyperparameter Optimization for Machine Learning Models Based on

Bayesian Optimization," *Journal of Electronic Science and Technology*, vol. 17, no. 1, pp. 26–40, Mar. 2019, doi: 10.11989/JEST.1674-862X.80904120.

[100] M. Bagheri, A. Bazvand, M. E.-J. of C. Production, and undefined 2017, "Application of artificial intelligence for the management of landfill leachate penetration into groundwater, and assessment of its environmental impacts," *Elsevier*, Accessed: Feb. 22, 2023. [Online]. Available: https://www.sciencedirect.com/science/article/pii/S0959652617303839

[101] M. Sakizadeh, "Artificial intelligence for the prediction of water quality index in groundwater systems," *Model Earth Syst Environ*, vol. 2, no. 1, Mar. 2016, doi: 10.1007/S40808-015-0063-9.

[102] R. Barzegar, J. Adamowski, and A. A. Moghaddam, "Application of wavelet-artificial intelligence hybrid models for water quality prediction: a case study in Aji-Chay River, Iran," *Stochastic Environmental Research and Risk Assessment*, vol. 30, no. 7, pp. 1797–1819, Oct. 2016, doi: 10.1007/S00477-016-1213-Y.

[103] "Mirabbasi, R., 2015. Application of artificial intelligen... - Google Scholar." https://scholar.google.com/scholar?hl=en&as_sdt=0%2C5&q=Mirabbasi%2C+R.%2C+2015.+Application+of+artificial+intelligence+methods+for+groundwater+quality+prediction.+In%3A+Nadir%2C+A.A.+%28Ed.%29%2C+Application+of+Artificial+Intelligence+Methods+in+Geosciences+and+Hydrology.+OMICS+Group%2C+Foster+City.&btnG= (accessed Feb. 22, 2023).

[104] M. Khaki, I. Yusoff, and N. Islami, "Application of the Artificial Neural Network and Neuro-fuzzy System for Assessment of Groundwater Quality," *Clean (Weinh)*, vol. 43, no. 4, pp. 551–560, Apr. 2015, doi: 10.1002/CLEN.201400267.

[105] A. Murat, S. Ö.-N. and E. Sciences, and undefined 2018, "Artificial intelligence (AI) studies in water resources," *dergipark.org.tr*, 2018, Accessed: Feb. 22, 2023. [Online]. Available: https://dergipark.org.tr/en/pub/nesciences/article/424674

[106] A. Wunsch, T. Liesch, S. B.-H. and E. System, and undefined 2021, "artificial neural networks: a comparison of long short-term memory (LSTM), convolutional neural networks (CNNs), and non-linear

autoregressive networks …," *hess.copernicus.org*, Accessed: Feb. 22, 2023. [Online]. Available: https://hess.copernicus.org/articles/25/1671/2021/

[107] S. Sengupta *et al.*, "A review of deep learning with special emphasis on architectures, applications and recent trends," *Elsevier*, vol. XX, 2019, Accessed: Feb. 22, 2023. [Online]. Available: https://www.sciencedirect.com/science/article/pii/S095070512030071X

[108] J. Samper, A. Naves, B. Pisani, J. Dafonte, L. Montenegro, and A. García-Tomillo, "Sustainability of groundwater resources of weathered and fractured schists in the rural areas of Galicia (Spain)," *Environ Earth Sci*, vol. 81, no. 5, pp. 1–15, Mar. 2022, doi: 10.1007/S12665-022-10264-5/FIGURES/8.

[109] L. R. D. Costa, R. T. Hugman, T. Y. Stigter, and J. P. Monteiro, "Predicting the impact of management and climate scenarios on groundwater nitrate concentration trends in southern Portugal," *Hydrogeol J*, vol. 29, no. 7, pp. 2501–2516, Nov. 2021, doi: 10.1007/S10040-021-02374-4.

[110] B. Pisani, J. Samper, and J. E. Marques, "Climate change impact on groundwater resources of a hard rock mountain region (Serra da Estrela, Central Portugal)," *Sustain Water Resour Manag*, vol. 5, no. 1, pp. 289–304, Mar. 2019, doi: 10.1007/S40899-017-0129-0.

[111] H. Moutahir, P. Bellot, R. Monjo, J. Bellot, M. Garcia, and I. Touhami, "Likely effects of climate change on groundwater availability in a Mediterranean region of Southeastern Spain," *Hydrol Process*, vol. 31, no. 1, pp. 161–176, Jan. 2017, doi: 10.1002/hyp.10988.

[112] T. Whare W-ananga, W. Hamilton, and M. A. Hall, "Correlation-based feature selection for machine learning," 2022, Accessed: Feb. 22, 2023. [Online]. Available: https://researchcommons.waikato.ac.nz/handle/10289/15043

[113] S. Maldonado and R. Weber, "A wrapper method for feature selection using Support Vector Machines," *Inf Sci (N Y)*, vol. 179, no. 13, pp. 2208–2217, Jun. 2009, doi: 10.1016/J.INS.2009.02.014.

[114] G. Chandrashekar and F. Sahin, “A survey on feature selection methods,” *Computers & Electrical Engineering*, vol. 40, no. 1, pp. 16–28, Jan. 2014, doi: 10.1016/J.COMPELECENG.2013.11.024.